1-1: The Structure and Chemistry of Asbestos Minerals.

by

E.J.W. Whittaker.
Department of Geology and Mineralogy,
University of Oxford,
Parks Road, Oxford.

Our knowledge of the structure of both chrysotile and of the amphibole fibres dates from the classic work of Warren and Bragg around 1930. Since that time knowledge has of course advanced steadily. In the case of the amphiboles, if knowledge is measured by the number of crystal structures that have been determined, then its increase seems to be going through a phase of exponential growth. But if our understanding is measured by the extent to which we can answer the questions that occur to us, then advances in understanding of the structure and chemistry of these minerals have been far from steady. Each advance in knowledge has tended to produce an immediate increase in the level of our understanding, but this has then tended to fall away again as new and unexpected facts have come to light, and new questions have presented themselves. Such fluctuations in the level of our understanding have been particularly apparent in investigations of the structure of chrysotile, as these have progressed from the chain structure of Warren and Bragg, through the ribbon structure of Warren and of Aruja, to later ideas on tubular structure and the difficulties of reconciling this with density measurements. The development of this work is reviewed as a background to some of the new information to be presented in other papers at the conference.

The vicissitudes in amphibole research have perhaps been less obvious than those in chrysotile research, but on closer examination they are found to be no less real. Earlier explanations of cleavage, fibrous character, and the relation of crystal symmetry to composition all now appear unduly facile. Recently determined structures, and the determination of cation ordering by spectroscopic methods pose new questions as well as providing new information about the factors responsible for the preferences of different ions for different sites in the amphibole structure. The relevance of current studies of the structure of holmquistite by the author, and of the synthesis of a 'hyper-sodic' amphibole $Na_4Mg_4Si_8O_{20}(OH)_4$ by Schreyer and Seifert will be discussed.

A persistent problem in the understanding of the amphibole minerals has been the sheer complexity of their classification, as a result of the wide range of ionic substitutions that occur in them. A recent proposal by the author to simplify their classification is described. This involves the avoidance of the concept of end-member

compositions whenever charge balancing, heterovalent, substitutions are involved. Classification is made on the basis of three variables, plotted along three orthogonal axes and representing charge above the minimum value in M_4 sites, $M_1 + M_2 + M_3$ sites and Si sites. Idealised compositions of named species then correspond to points with integral coordinates, and classification of real compositions is readily obtained by finding the nearest such integral point. Most calc-alkali amphiboles can be unequivocally classified in this way, though our knowledge of structural principles in the other series is at present inadequate to distinguish between some isomeric possibilities.

An attempt is made to relate structure to the differences between amphibole species in their behaviour in DTA and TGA procedures, and it is emphasized that confusion can only be avoided if primacy is given to structure in all questions of classification.

On the other hand a comparison of the various amphibole fibres with one another and with chrysotile suggests that structure, at the level of atomic arrangement, is not a primary factor in the control of fibre strength and that this is a problem for geology and geochemistry rather than crystallography.

1-2: Distribution of X-ray Diffraction Intensities from Faulted Cylindrical Lattices.

by

K. Toman* and A.J. Frueh.
Crystallographic Laboratory, McGill University,
Montreal, Canada.

Programs in Fortran IV language have been written for the calculation of the distribution of X-ray diffraction intensities of:

1) ideal cylindrical structures;

2) ideal cylindrical structure segments;

3) various models of mosaic structures derived from these ideal structures.

Calculations have been performed for some models of monoclinic chrysotile fibre of different mosaic structure.

The intensity distribution of the diffracted X-rays was measured on several chrysotile samples with widely varying physical properties, using a proportional counter with a balanced filter technique. Differences in scattering curves can be explained in terms of axial shifts and radial width of mosaic blocks.

* Nicolet Industries Fellow.

1-3: Spectroscopic Studies of Cation Ordering in Amphiboles.

by

R.G.J. Strens
Department of Earth Sciences,
The University, Leeds 2.

The hydroxyl group in the amphibole structure lies at the apex of a squat pseudotrigonal pyramid, the base of which is formed by three bivalent cations, two in crystallographically non-equivalent M1 positions, the third in the M3 position. In those amphibole solid solutions in which (M1,M3) are occupied by Fe(II) and Mg, a maximum of four narrow bands are observed (1,2) between 3700 and 3600cm^{-1}, corresponding to the stretching frequency of OH linked to $(Mg)_3$ = A, (Mg_2Fe) = B, $(MgFe_2)$ = C and $(Fe)_3$ = D.

The relative intensities of bands A to D have been used to determine (1-5) accurately (± 3% of the amount present) the Fe(II) contents of the (M1,M3) positions in asbestiform tremolite, amosite, crocidolite and riebeckite, in 12 natural members of the anthophyllite - cummingtonite - grunerite series, in 5 members of the tremolite - actinolite series, and in isolated samples of holmquistite, glaucophane, etc. Combined with Mossbauer data for the iron content of the (M4) site in the anthophyllite - cummingtonite - grunerite series, this has given the distribution of Fe(II) over M2,M4 and (M1,M3) in this series (fig. 1). The IR data alone give the distribution of Fe(II) in the tremolite - actinolite series (M4 filled by Ca) if the total Fe content is known from an analysis. The distribution of Fe over (M1,M3) is nearly random in these series, but Fe(II) prefers M1 in some alkali amphiboles.

Dehydration and (OH, F) exchange reactions in amphiboles can in principle be studied for the Fe(II) and Mg components separately by following intensity changes of the $(Mg)_3$ and $(Fe)_3$ peaks. Clustering of $(Mg)_3$ or $(Fe)_3$ can also be studied by comparing calculated (random mixture) and observed intensities of bands A to D.

Polymorphism (glaucophane I - II, anthophyllite - cummingtonite) of amphiboles will be discussed in the light of the observed cation distributions. Chemical and structural shifts of the OH stretching frequency, and extension of the IR work to other mineral insulators (talc, pyrophyllite, di- and tri-octahedral micas) will be reported briefly. (5)

Finally, spectroscopic work in the ultraviolet and visible regions has led to an understanding of the colour and pleochroism of certain strongly coloured amphiboles, micas and pyroxenes in terms of the band theory of solids. (5)

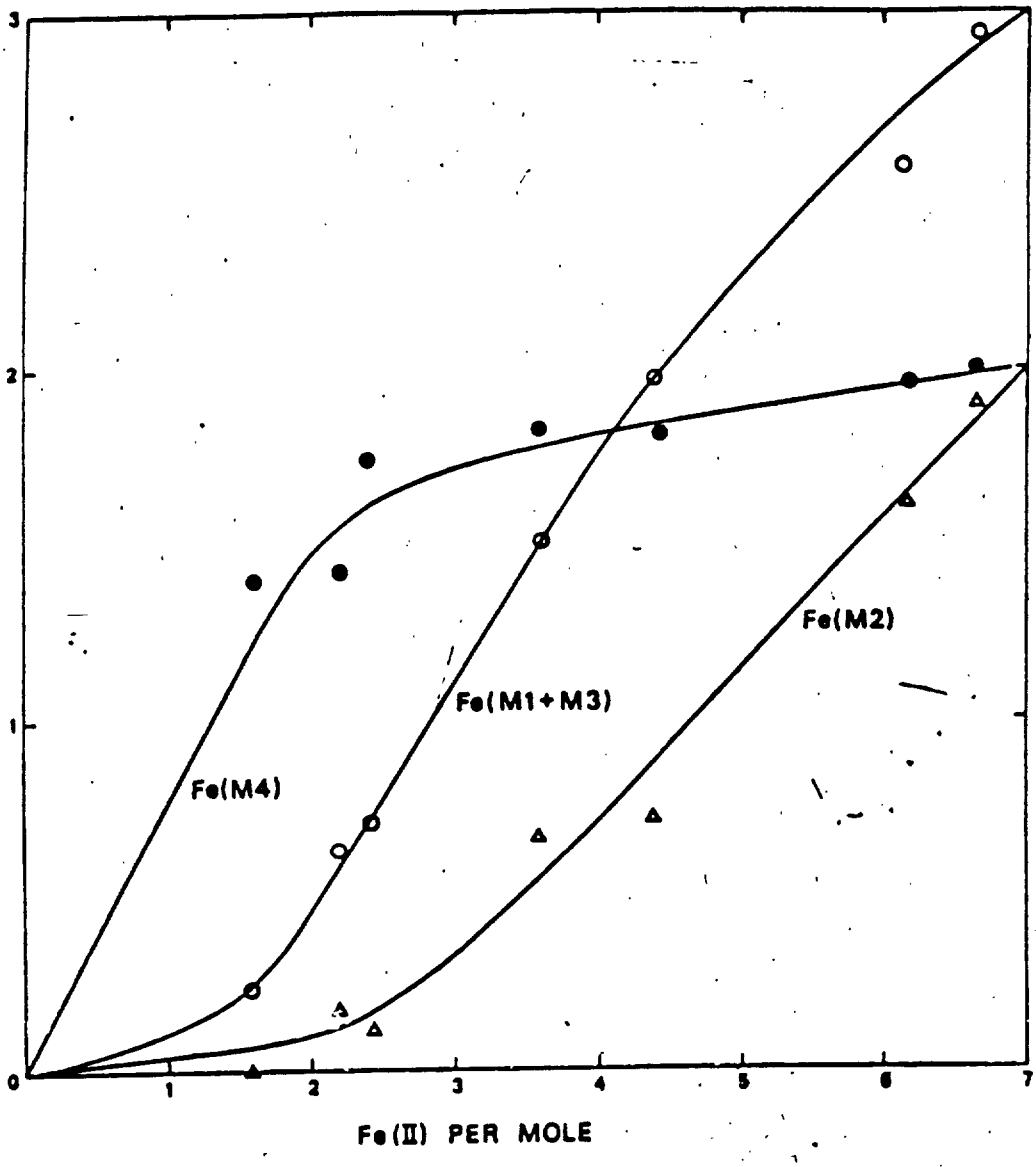

1. Burns & Strens, Science, 1966, p.890.
2. Strens, Chem. Commun., 1966, p.519.
3. Bancroft, Burns and Maddock, Amer. Min., in press.
4. Bancroft, Burns, Maddock & Strens, Nature, submitted.
5. Strens, unpublished work.

1-4 Mössbauer Study of Amphiboles.

by

H.J. Whitfield[1] and A.G. Freeman[2]
1. Department of Inorganic Chemistry,
University of Newcastle-upon-Tyne, England.

2. Department of Chemistry,
Victoria University of Wellington,
New Zealand.

The Mössbauer spectra of natural amosite and crocidolite and their thermal reaction products in oxidising and neutral atmospheres have been obtained. On the basis of the isomer shift and quadrupole splitting values, the assignment to sites of the iron atoms has been made. An attempt has also been made to elucidate the structures of the oxyamphiboles and of crocidolite anhydride.

The Mössbauer spectrum of Koegas crocidolite, $Na_2Fe_2^{3+}Fe_{2.6}^{2+}Mg_{0.4}Si_8O_{22}(OH)_2$, shows two broad bands at room temperature. These could be resolved into three symmetrical doublets, two of which were assigned to Fe^{2+} and one to Fe^{3+} on the basis of their isomer shifts. The relative intensities of the component peaks agree with the stoichiometry of the crocidolite sample.

The spectrum of oxycrocidolite, prepared by heating crocidolite in air at 450°C, shows a broad doublet with a quadrupole splitting of 0.95 mm/sec. This is assigned to Fe^{3+} ions residing preferentially on M_1 and M_3 sites (Whittaker's notation) with distorted octahedral environments.

Crocidolite anhydride was formed by heating crocidolite to 550°C in vacuo. The Mossbauer spectrum shows two distinct Fe^{2+} sites and one Fe^{3+} site. The Fe^{3+} ions are assigned to the M_1 sites with M_2 and M_3 sites occupied by Fe^{2+}. The quadrupole splitting value for Fe^{3+} is the same as that for Fe^{3+} in oxycrocidolite and on this account it is suggested that there is distorted octahedral environment about M_1 and M_3 ions in the anhydride. This is consistent with an inhomogenous mechanism for the dehydroxylation of crocidolite.

The Mössbauer spectrum of amosite (fibrous grunerite, $Fe_{5.5}Mg_{1.5}Si_8O_{22}(OH)_2$) shows four peaks. An inner doublet is assigned to Fe^{2+} ions in M_4 sites and an outer doublet to Fe^{2+} on M_1, M_2 and M_3 sites. On oxidation the ratio of intensities of the inner doublet to the outer doublet increases and a new pair of peaks appears which is assigned to Fe^{3+}. The quadrupole splitting for the Fe^{3+} peaks is similar to that observed for Fe^{3+} in oxycrocidolite and crocidolite anhydride. The change in the ratio of intensities of the inner and outer Fe^{2+} peaks suggests that the Fe^{2+} ions in M_4 sites do not take part in the oxidation and that electron transfer is along the cation chains rather than between cation chains.

--?: A New Serpentine Mineral Showing Diverse Strain-Relief Mechanisms.

by

F. Aumento.
Geological Survey of Canada, 601 Bootle Street,
Ottawa 4, Ontario, Canada.

A new and structurally unstable serpentine polymorph from the Tilly Foster Mine, New York State, is described.

The mineral (density 2.45 gm/cc) has an unusual morphology: it has a strong platy habit, with a perfect cleavage parallel to (001) and two good ones parallel to (100) and (010). Single crystal flakes, up to 5 mm across, can be bent with ease. Polysynthetic twinning occurs parallel to (001). The refractive indices are variable: n_α = 1.520-1.526, n_β = 1.522-1.528, n_γ = 1.528-1.535. Plates parallel to (001) extinguish at 7°-10° to the edges, and give a centred interference figure with a negative 2V between 83° and 90°.

The composition of the mineral is as follows:

SiO_2	41.70	Cr_2O_3	0.002	CaO	0.16	H_2O^+	13.19
TiO_2	0.07	B_2O_3	0.010	BaO	0.010	H_2O^-	1.45
Al_2O_3	0.31	MgO	40.83	K_2O	0.04	Total:	100.27%
Fe_2O_3	2.43	MnO	0.035	P_2O_5	0.03		

There is a small replacement of Si by Al, and Mg by Fe. However, more replacement, especially of Si by Al, would have been expected considering the large platy habit. Corrugation of the sheets, as described below, reduces the necessity of Si replacement to alleviate mismatching of the layers. The high Si:Mg ratio is also in keeping with corrugated sheets.

DTA and TGA data suggest similarities with chrysotile. Samples heated to 760-900°C produce forsterite ($Fo_{97.6}$). Above 1150°C protoenstatite is produced as the major phase, with minor forsterite. Above 1480°C forsterite becomes the major phase. Treatment with HCl produces an amorphous sample both before and after heating.

X-Ray diffractograms are similar to those of clino-chrysotile, with additional weak lines at 4.41 and 4.09Å. The pattern, except for the weak lines mentioned, can be indexed on a monoclinic cell with: a=5.320, b=9.222, c=7.277Å, and β=93.3°. However, a multiple 'a' or 'c' parameter is required for the indexing of the additional weak lines.

Single crystal photographs indicate that:

1. The mineral has a space group Cm, C2, or C2/m.
2. There is a superlattice effect similar to that found in antigorite, where the structure is modulated periodically in the 'a' direction, with a wavelength of 5.32x8=41.5Å. No change in this value has been observed between different crystals.
3. There is also a superlattice effect parallel to 'c', such that c=7.277x6=43.66Å, similar to that of the six-layer serpentines.
4. Whilst certain spots are sharp, others are elongated, in varying degrees, parallel to c*. On the basis of the extent of the elongation, the reflections can be subdivided into three types: (i) sharp reflections, (ii) reflections elongated by c*/2 along c*, and (iii) continuous streaks parallel to c* of uniform intensity, except for the falling off of the atomic scattering factor with increasing Sin θ/.

The serpentine layers making up the crystals are therefore displaced relative to each other by ± a/3 and ± b/3, with a probability of stacking mistake, α, of 0.4 for the 'a' direction and α = 1 in the 'b' direction.

Similar streaking could also be caused by random ± 60° rotation of each successive layer relative to its neighbours. However, serpentine layers individually corrugated parallel to 'a', on rotation would cause corrugations to show up in other directions, inhibiting stacking along 'c' with the repeat distance of 7.28Å. Corrugations would therefore have to be superimposed onto the layers after rotation, i.e., in the same direction with respect to the crystal as a whole.

Electron microscopy shows that the mineral exhibits two distinct morphologies, with a complete range of intermediate transitional morphologies. The original flakes, lying parallel to (001), are still apparent. These are often transversed by regularly spaced parallel lines. The plates are composed of a series of layers, each layer consisting of parallel-lying elongated laths. From the orientation of the component laths, it is seen that each layer is rotated with respect to its neighbours above and below. The layers break up at the edges into their consituent laths: the latter are scattered throughout the field of view. In turn laths show a tendency to curl up about an axis parallel to their length. Some of them exhibit this tendency in its initial stages, giving rise to crinkled edges. Other laths have gone a stage further, producing a close approximation to chrysotile tubes. End on views of the tubes are visible, with external diameters varying between 150 and 250 Å.

The plates give well orientated a*b* electron diffraction patterns, confirming the superlattice parameter parallel to a*. The laths show that curvature has taken place, whilst the tubes give patterns similar to the 'rotation' photographs of chrysotile tubes. The laths have therefore curved about the 'x' axis.

It is concluded that the mineral is an unstable polymorph of the serpentine group of minerals. It is a six-layer serpentine with stacking errors and layer modulations resulting in a crystal with superlattice-controlled 'a' and 'c' parameters. This configuration is stable only in its original macrocrystalline state, tending to break down into smaller, simpler units if assisted mechanically. Hence crystals break up in stages, at first forming thin corrugated plates. The latter part along weak corrugation joints, producing rods. Deprived of the satisfactory strain relief mechanism attributed to corrugation, the rods will necessarily be under strain due to the fundamental mismatching of the constituent silica tetrahedral and brucite octahedral layers. Unable to take up the strain in other ways, the rods resort to curling parallel to their elongation, finally producing more stable chrysotile-like tubes.

1-6 X-ray Microbeam Investigations of the Nature of "α-serpentine", "γ-Serpentine" and "Serpophite"

by
F.J. Wicks and J. Zussman
Department of Geology and Mineralogy,
University of Oxford,
Parks Road, Oxford.

The classification of the serpentine minerals has been based primarily on X-ray diffraction studies of single crystals and fibre bundles. The serpentine minerals responsible for the characteristic textures of serpentinized ultramafic rocks are too fine-grained to be studied by single-crystal methods and have thus in the past been studied by X-ray powder-diffraction techniques. This requires that the samples be crushed to a fine powder, making it impossible to determine the relationships of various serpentine minerals within the textures developed. The present application of a microbeam (50 um diameter) X-ray camera to the study of these textures has allowed the minerals to be studies in situ in thin section, so that the classification based on the single-crystal studies can be applied to the fine-grained minerals.

Mesh textures have generally been described as having rims of "α serpentine" (length-fast apparent fibres) with mesh centres of "γ-serpentine" (length-slow apparent fibres), or as having rims of "γ- serpentine" with mesh centres of "α- serpentine". These mesh-centres may or may not have an hour glass texture. In some other cases mesh centres have contained an isotropic material called serpophite. The microbeam X-ray photographs have shown that the "α-serpentine" forming the rims of some mesh textures is composed of lizardite platelets with their c axes (normal to platelets) perpendicular to the walls of the rims. "γ- serpentine", forming the rims of other mesh textures has been identified as chrysotile fibres with their a axes (fibre axes) perpendicular to the walls of the rims. The mesh centres, whether they have been called α serpentine γ- serpentine, or serpophite, have been found to be very fine-grained, randomly or very poorly orientated, masses of one of two minerals: lizardite in meshes that have lizardite rims, or chrysotile in meshes that have chrysotile rims. Exceptions to this general statement have been (a) the presence, within the mesh centres in two specimens of a phase giving a 14 Å reflection, in addition to the normal lizardite pattern, and (b) in one other specimen, the presence of fine veinlets of chrysotile fibre lying inside and parallel to lizardite rims, between the lizardite rims and randomly orientated lizardite mesh centres.

Brucite has been found, in one specimen, as an intimate intergrowth with lizardite platelets in "α-serpentine" rims.

[redacted]-Bastite, i.e. serpentine pseudomorphs after orthopyroxene, have been found to be most commonly composed of chrysotile, but alternate regions of chrysotile and lizardite can also occur on a coarse or fine scale within an individual bastite grain. The presence of both chrysotile and lizardite confirms earlier powder-method investigations.

The investigation is being continued with a more versatile microbeam camera and by electron microscopy to provide more detailed data. An electron microprobe will be used to look for chemical differences between mesh rims and mesh centres and possibly to verify the presence of brucite.

It is hoped that the orientations of the various components of the mesh textures can be related to the processes of serpentine formation.

1-7: THERMAL STUDIES OF WITTENOOM CROCIDOLITE IN VACUUM.

by

D.J. O'Connor and J.H. Patterson.
The Colonial Sugar Refining Co. Ltd.,
Research Laboratories,
Sydney, N.S.W. Australia.

Studies of the dehydroxylation of crocidolite from Wittenoom Gorge, Western Australia have been made using thermogravimetric, X-ray and infra-red techniques (Patterson, 1965, O'Connor and Patterson 1965). Dynamic thermogravimetric analysis under vacuum (0.03 u) reveals a weight loss of 0.6% to 525°C and a further weight loss of 1.9% up to 700°C. The infra-red spectra reveal that the latter weight loss is due to dehydroxylation while the former appears to be the loss of associated water.

Isothermal weight loss curves at 502, 522, 539 and 552°C are linear with time after a short period (½ hour) of rapid loss of associated water not removed by outgassing at 200°C. This simple zero order law is obeyed for about 50% of the reaction after which the observed rate of dehydration decreases (Fig. 1.).

At a higher temperature of 566, 577 and 591°C, the weight loss curves are parabolic in shape indicating a diffusion controlled reaction. This change in kinetics is also illustrated in Fig. 2, where the results are plotted as fraction reacted (a) versus relative time (t/t_{50}) and compared with several possible equations. The respective activation energies for the linear and parabolic reaction rates are 61 and 63 Kcal/mole suggesting that there is no marked change in the mechanism between 550 and 570°C. The change in kinetics therefore might logically represent a change in the rate controlling process with temperature.

During dehydroxylation in vacuum the four OH-stretching vibrations are not decreased uniformly and, in particular, peaks at 3633 and 3618 cm^{-1} are reduced relative to those at 3661 and 3649 cm^{-1} (Fig. 3). Based on the assignment of Burns and Strens (1966), this would indicate the preferential removal of hydroxyls with iron as nearest neighbours. This is therefore a further complication to the interpretation of the kinetic data and could contribute to a decrease of the rate as reaction proceeds.

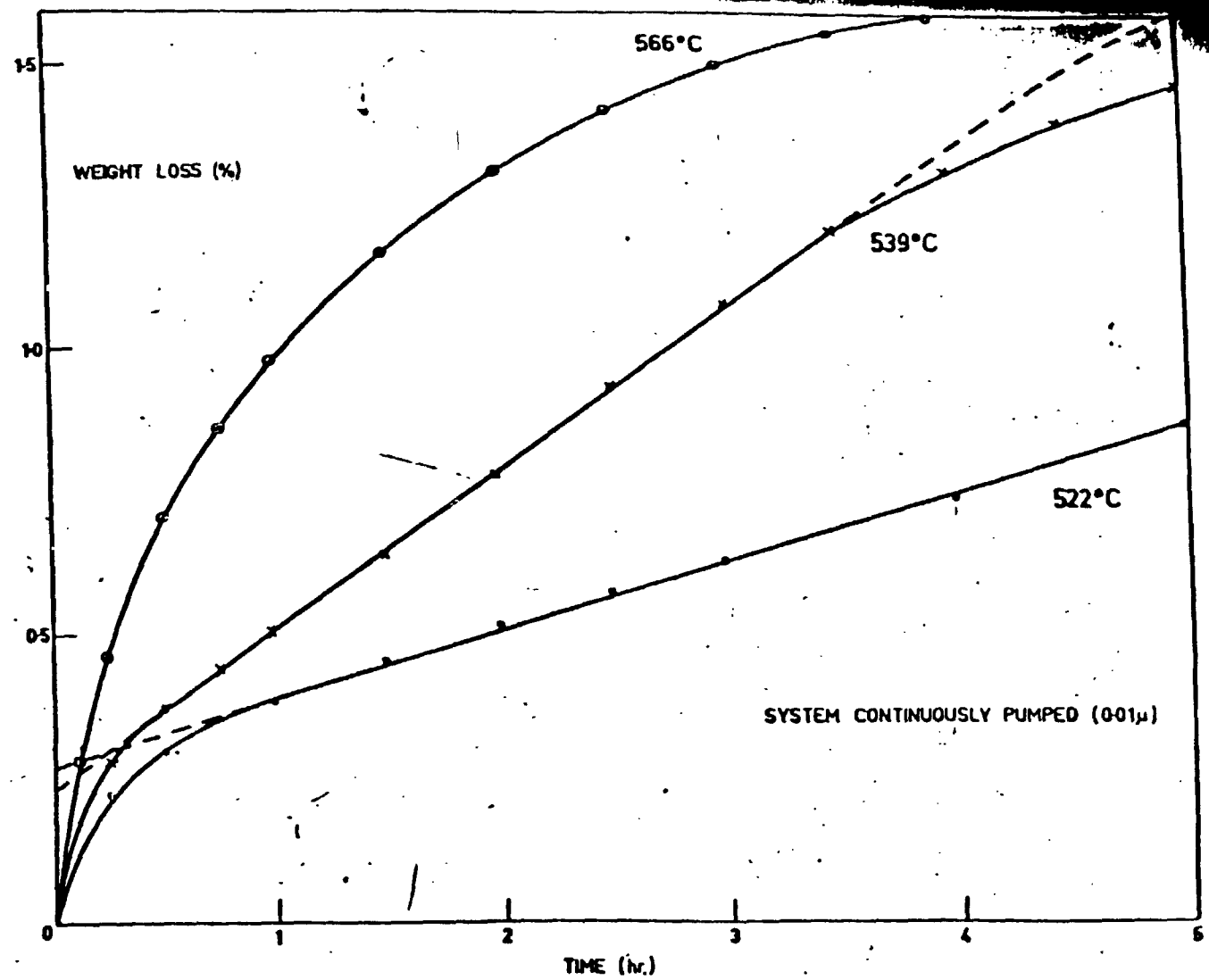

FIG. 1 ISOTHERMAL WEIGHT LOSS CURVES FOR WITTENOOM CROCIDOLITE HEATED IN VACUUM

The observed zero order kinetics can be taken to indicate that the dehydroxylation reaction proceeds as :-

(a) a surface reaction at constant rate. This is envisaged as involving two processes, viz.:

(i) Diffusion of protons and electrons to the surface of the crocidolite fibres, and

(ii) Elimination of H_2O from the surface of the fibres.

or (b) an interfacial reaction with the interface moving inwards at constant velocity on an effectively constant area.

For model (b) the equation for a cylinder reacting from the surface inwards may be more appropriate. This equation $1-(1-\alpha)^{\frac{1}{2}} = u/rt$ (where α is the fraction reacted, u the interfacial velocity, r the radius of the cylinder and t the time) does give a reasonable fit to the data up to 60 to 70% of reaction.

The observed rate of dehydroxylation falls below the theoretical equations after about 60% of reaction (Fig. 2), but this can be accounted for as a falling off in the supply of reactants for the surface reaction (model (a)), increased impendance of the dehydrated layer to the escape ofwater (model (b)), and variability in the resistance of specific hydroxyl groups to dehydration.

The change in kinetics observed at higher temperatures can also be explained, at least in qualitative terms, for both of the models discussed above. For the surface reaction model the rate of diffusion of reactants to the surface becomes rate controlling. For the interfacial model the diffusion of water through the product layer can become rate controlling.

The surface reaction model envisages the migration of protons and electrons to the surface and the formation and loss of water at the surface. To maintain charge balance inside the fibres the delocalisation of protons is balanced by the oxidation of Fe^{++} to Fe^{+++}. There is therefore little rearrangement of the internal structure and oxygen is lost from the surface. On the other hand, the interfacial reaction implies the formation of water inside the fibres and the diffusion of water through the dehydroxylated layer.

X-ray and infra-red studies reveal that the structure is retained after dehydroxylation with only slight disordering of the bulk of the structure (a thin decomposed surface layer would probably not be detected). All the structural water is lost from the crocidolite before the amphibole structure is destroyed. When this process is viewed in the wider context of the dehydroxylation of crocidolite and other amphiboles in air and in vacuum (Hodgson, 1965 and Patterson and O'Connor, 1966) it is felt that the surface reaction model may be the correct one.

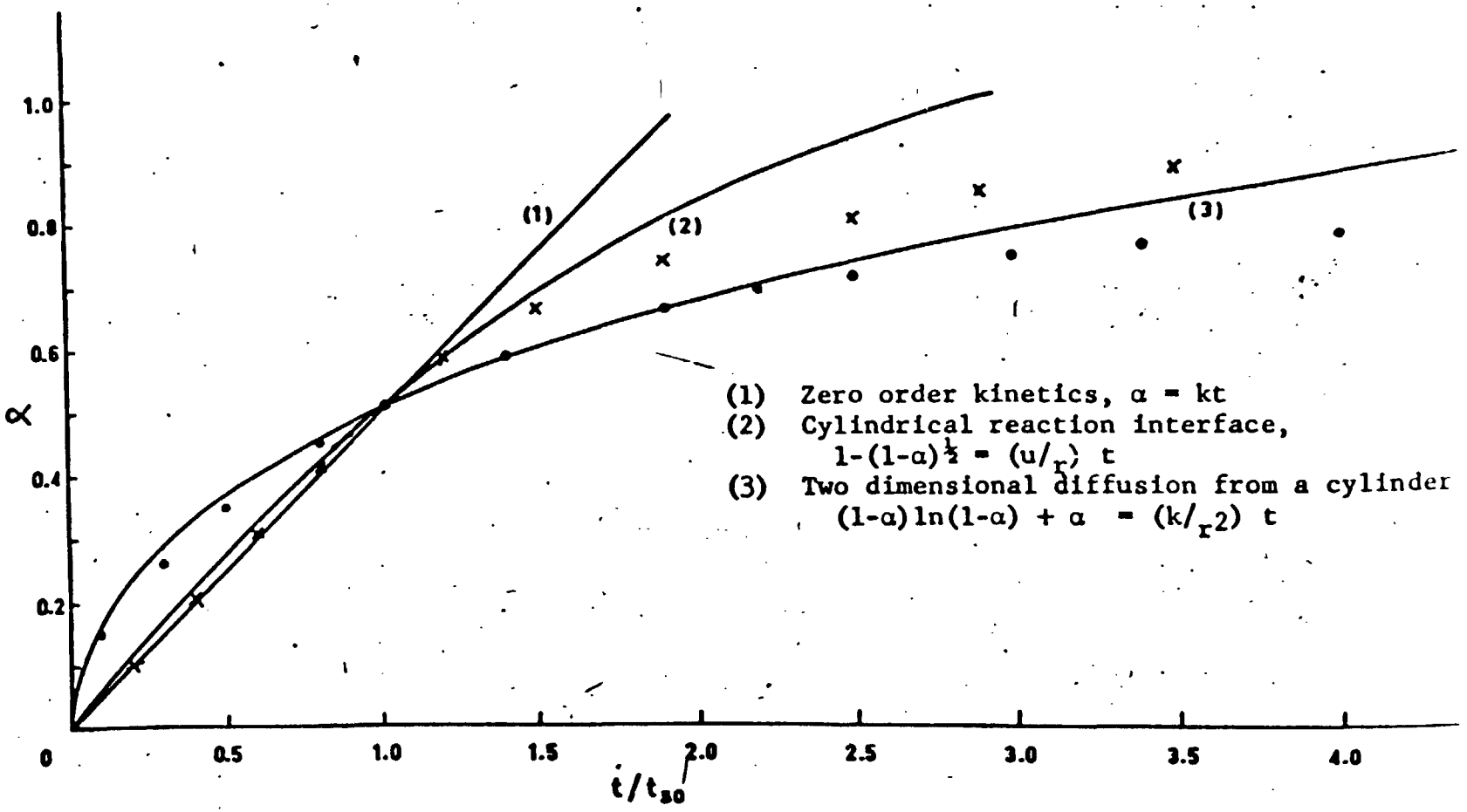

FIG. 2 FRACTION REACTED (α) VERSUS RELATIVE TIME (t/t_{50})

x Experimental results 502, 522, 539 and 552°C

• Experimental results 566, 577 and 591°C

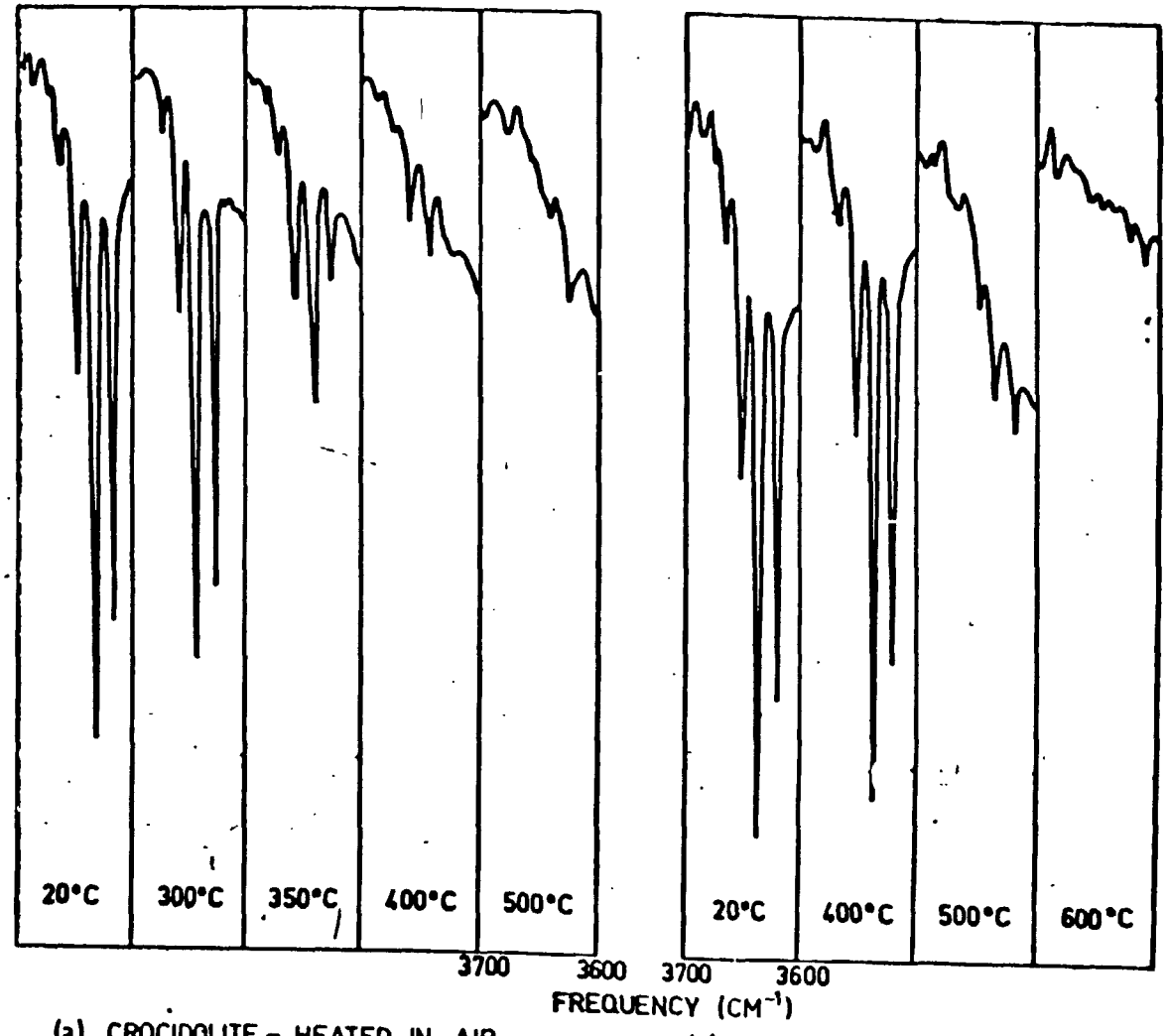

FIG. 3 OH STRETCHING VIBRATIONS (3700-3600 cm^{-1}) OF WITTENOOM CROCIDOLITE HEATED IN VACUUM AND AIR

ssible reactions are:

Within the lattice

OH^- (lattice) ---- O^{--} (lattice) + H^+ (mobile)
Fe^{++} (lattice) ---- Fe^{+++} (lattice) + e (mobile)

At the surface

OH^- (surface) + H^+ ----- H_2O
Fe^{++} + e ----- Fe^{++}

Overall reaction

$2OH^-$ ---- H_2O + O^{--}

These reactions are essentially similar to those generally accepted for the oxidation and dehydroxylation of crocidolite in air (Addison et al, 1962), except that oxygen is removed from the crystal surface rather than from the atmosphere.

REFERENCES.

Addison, C.C., Addison, W.E., Neal, G.H., and Sharp, J.H., J. Chem. Soc. (1962) 1468.

Burns, R.G. and Strens, R.G.J., Science (1966) 153, 890.

Hodgson, A.A. 'Fibrous Silicates' Royal Inst. Chem. Lecture Series (1965), No. 4.

O'Connor, D.J. and Patterson, J.H., Presented to the Ninth Conference on the Silicate Industry, Budapest (1965).

Patterson, J.H. Min. Mag. (1965) 35, 31.

Patterson, J.H. and O'Connor, D.J., Australian J. Chem. (1966) 19, 115[illegible].

1-8: The Relationship Between the Chemical Reactivity of Crocidolite and its Structure.

by

R.L. Thompson,
The Colonial Sugar Refining Co. Ltd.
Research Laboratories, Sydney,
N.S.W. Australia.

Wittenoom crocidolite fibres range in diameter from 0.5 to 0.15 microns with few falling outside this range. The procedure used to ensure that the fibres are separated employs severe agitation of a 0.2-0.5% slurry of crude fibre in water. High speed (50,000 r.p.m.) laboratory homogenisers and larger machines have been used for periods from 15-60 minutes depending upon the size and speed of the impeller. The slurry generally rises in temperature to about 70°C during this treatment. Fibres with length to diameter ratios of over 1000:1 are readily obtained.

Since the crocidolite so prepared is highly uniform, it is possible to calculate the physical effect of a given chemical reaction. The fact that 4% of the silica and 6% of the sodium are extracted by water in a Soxhlet apparatus indicates an attack to a depth of 1 and 1.5 unit cells respectively.

The attack by 0.2N sodium E.D.T.A. at pH 5.5 and 100°C is shown in Figure 1 to be diffusion controlled with some tendency for the layer of silica remaining from the reaction to disperse with time. As the cations are extracted, approximately one third of the released silica becomes dispersed in the solution while the remainder, having some of the original chain structure intact, remains close to the fibre. After three hours of reaction the attack has penetrated an average of 46 Å or 3-4 unit cells.

Less than 50% of the silica on the reacted fibres could be complexed by catechol indicating that it still retained some structure. All the silica on the surface readily dissolved in strong alkali. It was found to contain 4% w/w of water that was released over the temperature range 200-600°C. The silica esterified readily with butanol rendering the surface hydrophobic.

Raising the pH of the E.D.T.A. solution lowers the rate of reaction somewhat but the addition of calcium ions inhibits the reaction severely. It appears therefore that the E.D.T.A. group itself is directly involved in the attack on the fibres in contrast to the mechanism proposed by Mase (1959)

RATE OF CHEMICAL ATTACK ON WITTENOOM CROCIDOLITE

Figure 1

Sodium EDTA at pH 5.5

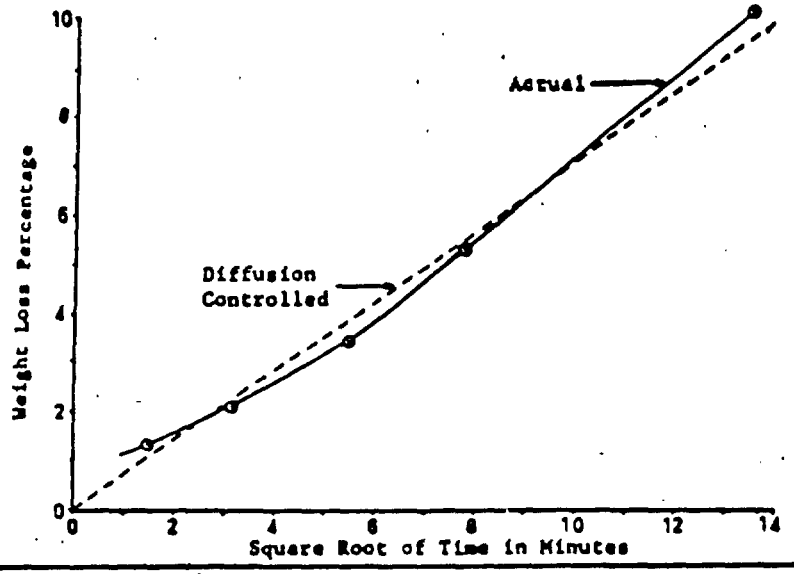

Figure 2

5N Hydrochloric Acid

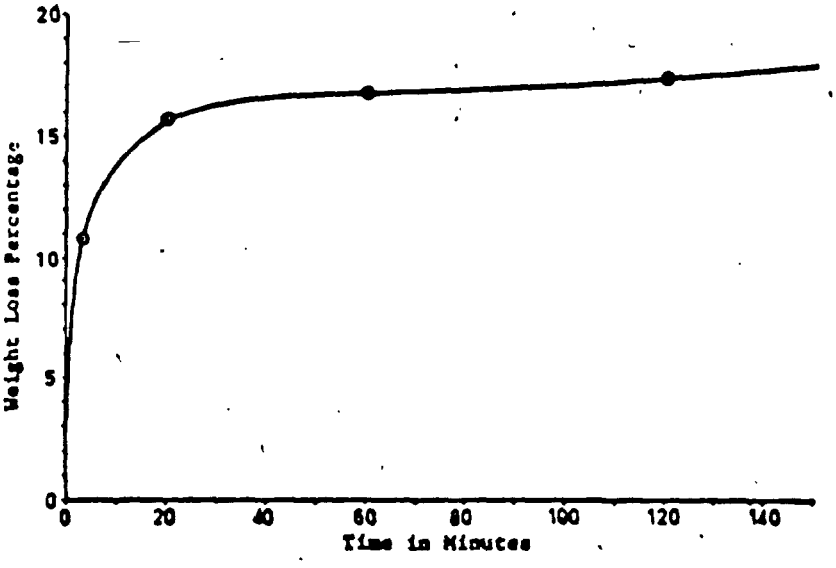

As would be expected from the observed susceptibility of crocidolite to complexing agent attack, the structure has no intrinsic resistance to acids. Even at pH3 and 100°C the metal atoms are removed from the outer half unit cells in two hours and the reaction is then only slowed down by the layer of silica chains that remain.

Figure 2 shows the rapid attack by 5N HCl at 100-110°C which, during the first three minutes, disrupts 20% of the structure, corresponding to a penetration of 57 Å or about 4 unit cells. The rate of reaction drops rapidly thereafter and there is less than twice the above penetration after 6 hours. This drop in rate may be ascribed to the formation on the surface of a tough coating of polymerized silica of low permeability. Only 15% of the released silica becomes dispersed in the solution in contrast to the behaviour during attack by E.D.T.A.

The polymerized silica has a water content of only 2% (200-600°C) and a surface area of 50 m^2/g. Its form is quite visible under the electron microscope. It is readily esterified by n-butanol, n-pentanol and benzyl alcohol, and is dissolved by boiling 2N NaOH.

Despite the rapid drop in reaction rate with time, prolonged attack by 5N HCl in a Soxhlet apparatus over some weeks is capable of removing all the cations from the crocidolite to leave a semi-fibrous mass of amorphous silica. The reaction is greatly accelerated at higher temperatures, e.g. $\frac{N}{10}$ H_2SO_4 at 300°C completes the reaction in a few hours.

In marked contrast to the effect of acids, alkalis at temperatures below 110°C have no more effect than water which can dissolve the silica from the outer unit cells. The surface of the fibres then becomes effectively composed of a continuous layer of metal atoms linked to their original octahedrally situated oxygen atoms.

The stability of this structure is understandable in terms of Radoslovich's work (1962) on the structurally determining effect of the metal atoms in layer structures. The tetrahedral layers are constrained to comply with the spacing requirements of the octahedral metal layer. The exposed metal atom structure on the attacked crocidolite is thus the stable part of the structure and prevents the dissolution of silica from between and below the octahedral layers. At temperatures above 100°C the structure weakens.

The sodium in the surface unit cells is easily extracted but is not replaceable by radioactive sodium. Only 10% of the surface unit cells take up sodium from 0.2N NaCl after an hour at 100°C. Some 30% of the surface sodium may be replaced with potassium, caesium or thallium. Cobalt is taken up to an amount equivalent to half the iron in the outer half unit cell, and calcium equivalent to half the magnesium.

The behaviour of amosite cannot be rationalised in terms of its structure as easily as that of Wittenoom crocidolite. It may be said nevertheless that its acid resistance is due principally to its larger diameter (0.5 to 2.0 micron) fibres since an attack to a depth of 1000 Å takes place under conditions that cause a penetration of only 100 Å into crocidolite fibres. Despite its smaller surface area of 5 m^2/g, amosite is severely attacked by boiling alkali as reported by Badollet (1951). This nitrogen adsorption surface area is four times the external surface area of the fibres so some faulting in the structure could be expected.

The resistance of amphiboles to chemical disintegration may depend mainly on the ability of the silica and metal atoms to retain their structure during attack and on the degree of faulting in the structure. The types of metal atoms and their positions in the structure determine the resistance to chemical attack only insofar as they affect this structural stability.

References.

Badollet, M.S., 'Asbestos, a Mineral of Unparalleled Properties'. Trans. Canad. Inst. Min. Metall (1951) 54, 151-160.

Mase, H., Kogyo Kagaku Zasshi, (1959) 62, 1716-18.

Radoslovich, E. Am. Mineral, (1962) 47, 599-616.
Ibid " 47, 617-636.
Nature " 195, 276

1-9: Hydrothermal Reactions of Crocidolite.

by

.. R.L. Thompson.
The Colonial Sugar Refining Co. Ltd.
Research Laboratories,
Sydney, N.S.W. Australia.

The work described was part of a general investigation into the properties of Wittenoom crocidolite undertaken with the aim of gaining a better understanding of the material for possible new applications. Work at temperatures up to 100°C showed that apart from disintegration by acids, chemical reactions on crocidolite were confined essentially to the surface which behaved as a fault free silicate surface.

Because of the exceptional stability of the basic crocidolite structure to alkali attack, it has been possible to carry out a wide range of controlled reactions in alkaline solutions at temperatures between 100 and 550°C under pressure. In order to retain the tensile strength of the fibre most work was confined to temperatures below 350°C.

Many of the reactions lead to a breakdown of the structure at the fibre surface with a concurrent synthesis of new minerals on the surface as coatings or particles. 10 sodium and potassium hydroxides at temperatures from 100 to 400°C progressively disintegrate the structure. Potassium hydroxide leads ultimately to the production of a mass of fine crystals. This is in contrast to sodium hydroxide at 400°C which results in the synthesis of a fibrous mineral having the same colour and fibre diameter as crocidolite but differing in crystal structure.

As the crocidolite structure is broken down by the alkali, the silica will react with many reagents if they are held in solution or dispersion. For example, reaction with alkaline sodium plumbate at 300°C leads to deposition of 300 Å lead containing crystals or coatings onto the fibre surfaces over a wide range of reagent concentrations. Sodium vanadate reacts similarly as do most elements capable of forming insoluble silicates. These products together with those formed using dispersions of nickel and cobalt hydroxides may have applications as catalysts. The surface area of the nickel containing coating was 100 m^2/g.

In view of its commercial importance, the reaction of crocidolite with lime at 300°C was investigated. The production of insoluble material was found to be effectively completed in a few minutes and the main product consisted of 1 micron spheres of amorphous material firmly attached at intervals to the fibres.

The physical form of the fibres is affected by some reagents such as alkaline sodium phosphate which causes many fibres to become markedly curved. The 50 Å crystals deposited from sodium zincate and some other reagents are capable of decorating cleavage planes parallel to the fibre axis. Actual cleavage of 1000 Å fibres into five or six smaller fibres occurs quite frequently at 300°C and is promoted by sodium borate and zirconate. No other means for reducing crocidolite to 150 Å fibres is known.

The most interesting group of products were those formed by reaction with alkaline aluminates. A range of selective ion-exchangers were produced by varying the alkali used in the reaction and optimising the temperature and reagent concentrations. Barium aluminate gave exchangers with a high selectivity for divalent cations and a capacity of 0.8 m eq./g of fibre. Sodium aluminate yielded materials with greatly enhanced capacities of up to 2 m eq./g for monovalents over divalents (0.2-0.5 m eq./g) with some preference for caesium. Under suitable conditions potassium aluminate produced a highly selective caesium exchanger similar to clinoptilolite with a capacity of 1 m eq./g.

The ion-exchange materials were in the form of 100-200 Å coatings on the fibres. Their rate of exchange was typical for zeolites but the coating contained only 5% water in contrast to the 30% commonly found in zeolites. No internal surface area could be detected in the coatings using nitrogen adsorption.

The severity of the attack by alkali aluminates is exceptional and was exceeded, during the investigations described, only by acids. An increase in the temperature of reaction to 350°C typically led to complete disintegration of the fibres and to the formation of fine crystals of varying shapes and colours.

2-1: Physical Properties of Asbestos Minerals and their Technical Applications.*

by
M.S. Radollet.
Health Research Institute,
Fairleigh Dickinson University,
Madison, New Jersey, U.S.A.

In fundamental studies on asbestos minerals the selection of samples and the history of the deposit can furnish valuable clues on the physical properties of the fiber and its use in industry. This is then followed by the proper preparation of the samples for the many physical and chemical tests involving the identification and quantities of mineral impurities in the crudes and drill cores.

Actual milling plants for asbestos separate and grade the fibers to meet standard tests but they do not eliminate all of the objectional associated minerals that may affect the physical properties of the fiber when used in some products such as textiles, floor tiles, plastics and many others. Attention to trace elements in samples of asbestos may be of particular importance in biological studies for the effects of asbestos on tissue, particularly in tests for carcinogenicity. Also if trace elements are present during the filtration of wines, beers, blood plasmas, and pharmaceuticals they may be objectionable.

The foreman of any plant producing asbestos products should know the true quantities of pure asbestos present so that he can vary his formula to give a satisfactory end product with the proper physical properties to meet the specifications.

Rate of filtration or the elimination of water in an asbestos slurry is an important property which will govern production of a large quantity of asbestos products such as papers and asbestos cement products.

A mill survey covering samples taken at different stations over a period of time can point out the objectionable equipment that is damaging the fibers physical properties. Then it is a process of elimination or regulating the equipment to improve the fibers properties.

The slimy effect of soft chrysotile fibers can be eliminated by heat treatment, acid treatment, or by the addition of sodium silicate. Wetting agents can be helpful in improving the water elimination by filtration. Dispersing agents can prevent settling of the stock in the vats during the production cycle. The use of any of these agents must be carefully controlled.

* This work was supported in part by the U.S. Public Health Service Grant OH-00252 from the Division of Occupational Health.

The electrical properties of chrysotile can be improved by a soap treatment and by the elimination of magnetite and other mineral impurities.

By taking advantage of the electropositive charge on chrysotile it is possible to reduce fiber losses in wet processes by adding a negative charged mineral. In the production of some types of cellulosic papers the addition of electropositive chrysotile will help in retaining the clays or titanium dioxide and at the same time furnish a high surface area. Papers that are to have rubber latex deposited on the furnish are greatly improved by the addition of the positivecharged chrysotile that helps to hold the latex during the sheet formation.

Air polution problems are important today and it requires the collection of large quantities of air containing the air floated particles. If asbestos is involved it will require micro test methods to identify the fibers in the presence of contamination such as fly ash, metallic particles from metallurgical and smelting plants. It can also involve a bag house installation using asbestos, glass or cotton or wool with a precoat of fine particle sized asbestos to aid the bags in retaining the solids.

In many miscellaneous applications of asbestos their physical properties are important such as the effects of grit, whiskers, unopened fiber bundles, micaceous materials, brucite, other closely associated minerals, bulk, density, surface area, texture, flexibility and tensile strength. Such products are caulking compounds, sprayed undercoatings, thermal insulating cements, wall joint fillers, paints, plastics and molding powders.

The physical properties of asbestos minerals are many fold and it is the decision of the plant manager to select the proper type of asbestos to meet his requirements.

Many of the important physical properties of asbestos fibers are discussed and examples of their applications are shown in the production of many products.

2-2: Chemical and Physical Characteristics of Soft and Harsh Chrysotile.

by

Arthur M Langer[1] and Paul F. Kerr[2]

1. Department of Community Medicine,
Mount Sinai School of Medicine,
New York.

2. Department of Geology,
Columbia University, New York.

Representative samples of soft and harsh chrysotile have been collected from a large commercial asbestos mine in Eastern Canada where veins of the mineral types are intimately associated in time and space. Geologic occurence of the fiber types suggests that they have originated because of minor chemical and/or physical variation in their environment during formation.

These materials are compared chemically and physically with their wall-rock host as well as with each other. Chemical analysis of the chrysotile types include trace elements as well as bulk oxide components. Analyses of bulk and size and magnetic sample splits are given. Electron photographs, x-ray diffraction, differential thermal and infrared spectral data are also given and some basic differences in the fiber types are proposed. Fiber photographs suggest possible structural differences between fiber types.

2-3: An Investigation of the Tubular Structure of Chrysotile Asbestos by Electron Microscopy and Electron Diffraction.

by

A.L. Rickards
Chemical Research Department,
Turner Brothers Asbestos Co. Ltd.,
Rochdale, Lancashire.

Many workers have published electron micrographs of cross fibre fibrils illustrating an electron light region along the long axis of the crystal and have interpreted this effect as evidence for a hollow tube structure. It has also been suggested by several workers, from electron microscopy evidence and surface area measurements that if a tubular structure does exist it is filled with some amorphous material.

Whittaker (1) has shown by x-ray diffraction studies that the structure of chrysotile conforms to the model of a single crystal hollow cylinder with an outside diameter of approximately 300Å and an inside diameter of approximately 90Å.

EXPERIMENTAL

Specimen Preparation.

Unopened cross fibre specimens from Rhodesia (Shabani Mine), British Columbia (Cassiar Mine), Quebec (Thetford Mine), Swaziland (King Mines) have been examined. A Union Carbide product with a high surface area was also examined, this sample being considered to have originated from Central California.

Electron Microscopy.

The appearance of the tubular effect in chrysotile was investigated and related to variations in the position of focus. A fibril was defined as being in focus when no interference fringe was visible about its projected diameter, and in this condition no tubes were visible in the cross fibre specimens examined. At a setting with the specimen out of focus, above the focal plane, the 'tubes' became visible. In contrast, a large proportion of fibrils from the Union Carbide product showed the electron light region when in focus.

At the magnifications (greater than 55,000X) necessary to properly define focus, the condenser system of the microscope was focussed to give the smallest possible beam diameter in order to produce sufficient brightness at the viewing screen. Under these conditions electron beam damage rapidly transformed the single crystal fibrils into an amorphous state, i.e. when no sharp diffraction spots or rings were visible using 100 Kv. During this transformation the fibrils became distorted but still retained their original dimensions. With the normal cross fibre chrysotile, an electron dense region developed along the long axis of the fibre, whereas those fibrils from the high surface area product, which originally exhibited the electron

light region when properly focussed, retained the electron light region when amorphous, even after prolonged irradiation.

After reducing the single fibrils to the amorphous state, the specimen was then heated in the microscope and several exposures taken as the temperature rose, recording alternately the diffraction pattern and the magnified image. At a temperature estimated to be about 600°C, diffraction rings began to appear indicating a recrystallisation of the amorphous fibrils. The lattice spacings of this first crystalline phase correspond to those of magnesium oxide. On further heating a second phase appeared which is being interpreted as possibly forsterite and work will continue to make a more positive identification of this phase. Both types of specimen, i.e. cross fibre chrysotile which exhibited the electron dark zone and the commercial product which retained the electron light region in the amorphous state, were subjected to this heat treatment. Both types gave the magnesium oxide pattern and a similar final pattern.

DISCUSSION.

It is suggested that the tubes are filled with a non-crystalline material, i.e. not detectable with 100 Kv electrons; as no evidence can be provided by x-ray and electron diffraction for the presence of any structure other than that of single crystal chrysotile in undamaged fibres. Considering that about 10% of the volume of a fibril can be attributed to the tube, then if this tube is packed with any non-chrysotile material it would be expected to be detectable by diffraction either in a single crystal or polycrystalline form; in fact no other phase is detected. If the material were chrysotile in a polycrystalline form it should also be detectable in the fibre diffraction patterns as a superimposed ring pattern. A mosaic single crystal plug would be undetectable by diffraction of the undamaged fibril but would obscure the effect of the tube in the single crystal fibre. Also if this plug were a single crystal of chrysotile it would be expected to behave in an identical manner to the chrysotile fibril during beam damage and thus would not manifest itself as anelectron dark zone at the amorphous stage. Any filling present is therefore presumed to be amorphous.

CONCLUSIONS.

1. The contrast in electron micrographs of chrysotile is sensitive to changes in focus.

2. Chrysotile is extremely susceptible to electron beam damage.

3. Chrysotile fibrils conform to the x-ray model of tubular cylinders, and in general, are filled with an amorphous material.

REFERENCE.

1. Whittaker, E.J.W. 1956 'The Structure of Chrysotile (ii) Clino Chrysotile' Acta. Cryst. 9, 855-856. 1957 'The Structure of Chrysotile (v) Diffuse Reflections and Fibre Texture' Acta. Cryst. 10,149-155.

2-4: The macroporosity of asbestos fibres.

by

M. della Faille
Dr. en Sciences, Chargé de Recherches,
S.A. Eternit, Kapelle-op-den-Bos,
Malines, Belgium.

Many workers, such as Pundsack, Young & Healey, Nanman & Dresher, Fripiat, and della Fraille have given results concerning the porosity of asbestos fibres.

The methods used in the present work are based on two techniques: N_2 adsorption isotherms, and the mercury porosimeter. The first gives information on pores having diameters in the range 20 - 400 Å, while the mercury porosimeter allows one to detect pores having diameters of 150 Å - 100 u.

Various fibers, including Cassiar, Jeffrey, Coalinga, and Corsican and Russian chrysotiles, have been studied in this way. All these fibers were water washed materials of various lengths, treated at different temperatures.

The pore size distribution (150 Å to 100 u diameter) may be divided into two domains, characterized by pore diameters of 150 Å - 15 u and 15 u - 100 u respectively. The pores in the first range are mainly due to the bundle porosity, while those in the second are more dependent on the fibre length. The corresponding void volume is usually between 0.2 and 0.8 cm^3 g^{-1}. There is no relation between the surface areas (B.E.T.) and the volume of the voids between the fibre bundles. However, it seems that the apparent density of the bundles becomes higher when the external fiber diameter is smaller. This relation can be explained by assuming that the cohesion is better between fine fibers than between coarser fibers.

Other relations between microporosity (water and nitrogen) and macroporosity (mercury) are given, which are in good agreement with some mechanical properties of the fibers.

2-5: The Physical Nature of Wittenoom Crocidolite.

by

J.H. Patterson and R.L. Thompson
The Colonial Sugar Refining Co. Ltd.,
Research Laboratories, Sydney,
N.S.W. Australia.

Wittenoom Crocidolite fibres fall in the diameter range 0.05-0.15 micron. The surface area of fully fiberised crocidolite measured by nitrogen adsorption is 14.8 m^2/g which corresponds to an average fibre diameter of 0.082 micron, in good agreement with electron microscopic examinations. Cape Blue asbestos has a far wider range of fibre diameters and a surface area of only 10.7 m^2/g using the same preparation and measuring techniques.

Sawn blocks of Wittenoom crocidolite have surface areas around 5 m^2/g which increase to between 7 and 8 upon teasing out the fibres. Fiberisation in the dry state as employed for asbestos cement manufacture does not increase the surface area. A sample of Cape Blue commercial fibre tested at 4.85 m^2/g. Whilst this surface area is available to nitrogen adsorption, the rate of diffusion to and from the surface for chemical reaction is halved. The high acid resistance shown by some fibres would be partly due to this inhibited diffusion.

Grinding crocidolite in an agate mortar results in the formation of agglomerates that appear as transparent crystals under the optical microscope. Electron microscopy reveals that the agglomerates are composed of broken fibres of roughly the original diameter. The surface area was 25 m^2/g indicating that the fibres have been broken both normal and parallel to their length. Compression of fully fiberised crocidolite at 150,000 p.s.i. average pressure caused a rise in surface area to 20 m^2/g and the formation of fine particles that readily peptized in water. The suspension was coagulated rapidly by the addition of a small amount of lime. Neither grinding nor compression assists the 'subfiberisation' to the 150 Å fibres observed for hydrothermally reacted crocidolite. Oxidation and reduction at similar temperatures, i.e. up to 350°C, do not affect the minimum fibre diameter or the surface area.

Density measurements have shown that the porosity of crocidolite blocks is approximately 10%. The volume of the blocks was determined by geometric measurements, by mercury displacement and by the use of a pycnometer. Densities ranging from 3.0 to 3.4 g/cc. have been obtained depending upon the technique and the extent of degassing. Fully fiberised crocidolite in equilibrium with air of 60% R.H. had a density of 3.29 g/cc. This density is well below the X-ray density of 3.45 g/cc indicating that the surface is covered with several monolayers of water. Two of these layers, equivalent to 0.8% w/w of water, are lost at 100°C.

Nitrogen adsorption-desorption isotherms recorded on blocks, teased fibre bundles, commercially fiberised and fully fiberised crocidolite are shown in Fig. 1. The adsorption isotherms are of type II on Brunauer's classification as has been commonly reported for various types of asbestos. Equilibrium is attained rapidly for the fiberised materials but only very slowly on the blocks. With blocks, low surface area results are obtained if insufficient time is allowed for adsorption.

Hysteresis is very marked during desorption of partially fiberised samples but is not observed with fully fiberised material. When hysteresis is observed there is a pronounced step in the desorption isotherm between relative pressures of 0.4 and 0.6 (see Fig. 1). This indicates a very narrow distribution of pore size about an effective radius of 20Å and accounts for about 70% of the total porosity. The step in the desorption isotherm decreases as the degree of fiberisation is increased, indicating that the pores are between fibres or fibre bundles rather than in the individual fibres themselves. In contrast the sample of Cape Blue asbestos exhibited little or no hysteresis.

The observed hysteresis loops appear to be of type-B according to the classification of de Boer (1958) combined with an isotherm of type II which becomes increasingly dominant with increased degree of fiberisation. Hysteresis loops of type-B can be expected from open slit-shaped capillaries with parallel walls or from cylindrical capillaries with very wide bodies and short narrow necks ('ink bottles'). The observed 20Å effective radius can therefore be taken as the distance between parallel faces of individual fibres (or fibre bundles) or the radius of voids between fibres leading into much larger cylindrical pores. The parallel plate model does not appear to be consistent with the observed porosity of 10-12% and hence the pores are probably of the 'ink bottle' type.

Since the surface area of fibre blocks is one third, and that of teased fibres one half of the total surface area, the fibres probably occur as bundles of four or more in close contact. The thermal conductivity normal to the fibres ranges from 20 to 40% of that in the axial direction so the fibre bundles are not isolated but appear to be attached at intervals along their length. This configuration is consistent with the 'ink bottle' model of the pores.

These observations help to clarify the problem of fiberisation. Teasing out the fibres to make available 50% of their ultimate surface area is achieved with little effort. Further dry beating separates and shortens the bundles. Separation of the fibres in the bundles requires a great deal of work and can be achieved only at the expense of fibre length.

The authors thank Mr. F.B. Dwyer for his work in measuring the thermal conductivities and some of the densities of fibre blocks.

REFERENCES. de Boer, J.H., 'The Structure and Properties of Porous Materials'. Proc. 10th Symp. Colston Res. Soc., (1958) 68.

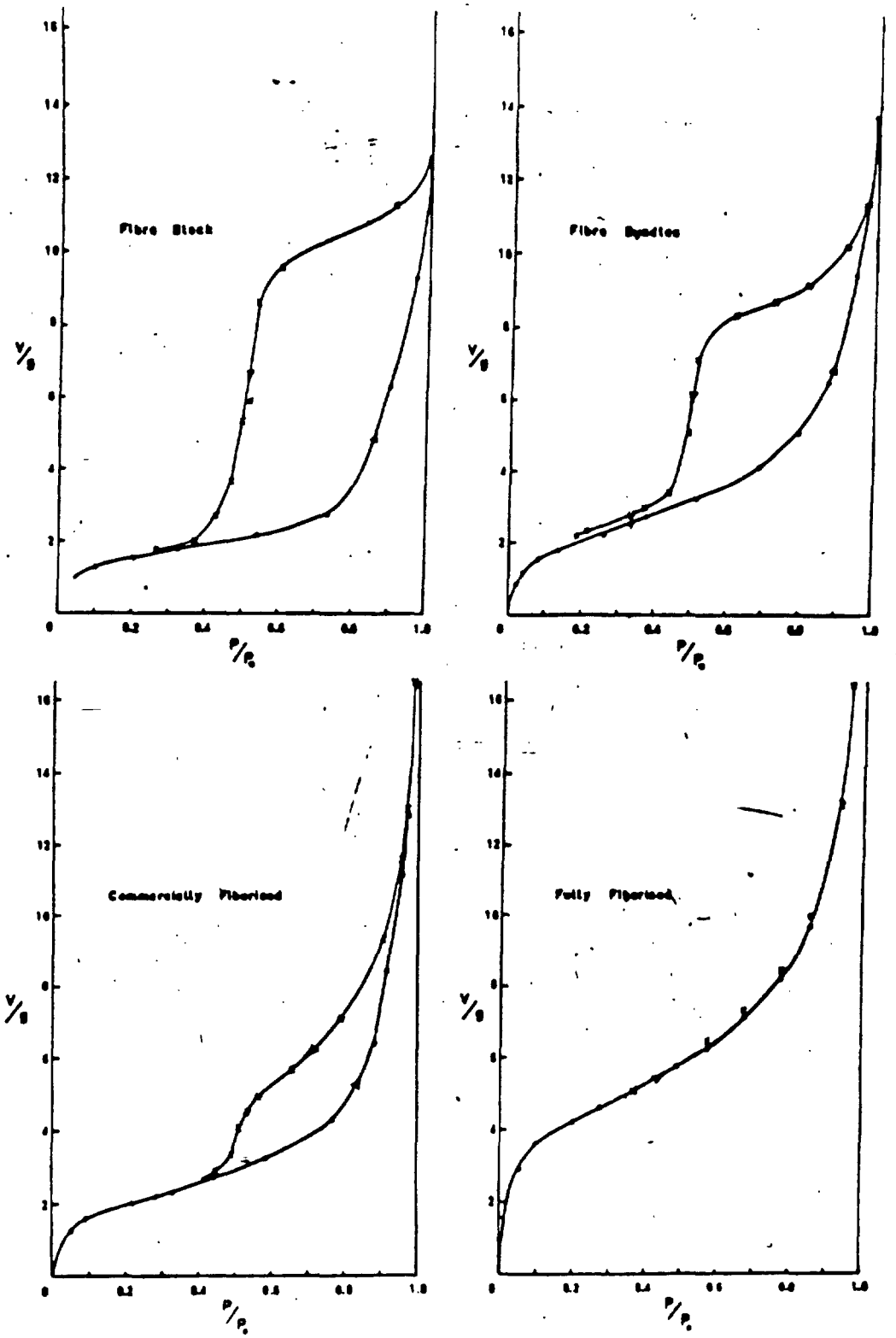

FIG. 1 NITROGEN ADSORPTION - DESORPTION ISOTHERMS FOR WITTENOOM CROCIDOLITE

Volume of gas adsorbed (cc/gm) versus relative pressure (P/P_o)

• Adsorption Isotherm

x Desorption Isotherm

2-6: Surface Chemistry and Organic Derivatives of Chrysotile Asbestos.

by

J.J. Fripiat, E. Mendelovice and C. De Kimpe
Laboratoire de Chimie Minérale,
The University of Louvain,
92, Avenue Cardinal Mercier,
Heverlee-Louvain, Belgium.

When samples of chrysotile are attacked by acid solutions, the magnesium cations are removed, and the surface areas are increased by more than twenty times, but the tubular morphology still persists. The tubular residues are 'X-ray' and 'electron diffraction' amorphous. The pore-size distribution functions are shifted towards larger pore diameters. Under these conditions, the textural behavior is considered as resulting from the presence of disordered silica particles randomly distributed in an apparently intact cylinder. It will be shown that it is possible to replace the magnesium - containing octahedral layers by ordered layers containing methylsilicon radicals. In this case, the tubular morphology is destroyed by unrolling of the sheets. The resulting material is X-ray amorphous, but the ordering of the silica is clearly shown by electron diffraction patterns. Surface areas are as high as after the acid treatment, but the surface properties are completely different. The hydrophobic character is normally well marked.

2-7: Adsorption of Organics by Chrysotile Asbestos.

by

T.J. Weeks, Jr. and J.P. Leineweber
Johns-Manville Research & Engineering Center.
Manville, New Jersey, U.S.A.

Fundamental data on the interaction of organic compounds with chrysotile asbestos and related compounds will be presented. These data are primarily in the form of adsorption and desorption isotherms from both the vapor and liquid phases.

The adsorption from the liquid phase has been studied from binary systems using a Brice-Phoenix differential refractometer to measure changes in the solute concentration. This instrument is capable of measuring changes in refractive index as small as 3×10^{-5}. Compounds which are representative of the different classes of organic molecules have been studied, including normal and branched chain hydrocarbons, alcohols and aromatic compounds. Aldehydes and ketones were not included in this preliminary study because of the complicating factor of base catalysed condensations which can take place in these systems.

In addition to the effect of solvent type, i.e., polar versus non-polar, on the adsorption isotherms, the effect of the degree of 'openness' of the fibers and their thermal history will be discussed. Comparisons will be made between fibers in equilibrium with atmospheric moisture, fibers heated to remove adsorbed water, and fibers which have been subjected to various degrees of dehydroxylation.

Adsorption on chrysotile asbestos will also be compared with adsorption on various related materials, such as, serpentine rock, magnesium hydroxide, magnesium oxide, and silica.

Adsorption from the vapor has been determined for many of the same compounds studied from the liquid phase. In this case the adsorption-desorption isotherms were determined for the pure compounds by standard volumetric techniques.

2-8: The Tensile Strength of Asbestos Fibres.

by

D. Burman
Cape Asbestos Fibres Limited.
Harts Lane, Barking, Essex.

The paper consists of a summary of the tensile strengths obtained for samples of all the major types of asbestos fibres, including values for similar types from different locations. The paper also includes details of tensile strength determinations on asbestos fibres which have been heated to various temperatures. This new work on tensile strengths is based on an examination of asbestos fibre strengths carried out by R. Zukowski & R. Gaze[1]. The apparatus used for this present work is, however, considerably more accurate and the results obtained are correspondingly subject to less experimental error.

The fibres were tested on the Techne Micro Tensile Testing machine originally designed by Marsh[2] for examining metal whiskers, but ideally suited for the testing of small asbestos fibres. All tests were made on fibres of 4mm length, generally having a cross-sectional area of $1\text{-}3 \times 10^{-6}$ cm^2, corresponding to an equivalent diameter of 10-20 microns. Almost all the fibres tested were selected from ore samples, thin slivers being pulled off and further subdivided by tweezers. The cross-sectional area of each fibre was determined from measurements of its weight, length, and density. Each fibre was weighed to 0.1 microgram on an Oertling Decimicro balance. The length of the fibre was measured using the travelling microscope incorporated into the tensile testing machine. The density of the amphibole fibres had in most cases been previously measured. The value for chrysotile and the remaining amphibole fibres was taken from text book data.

From Table I the following points emerge:-

1. The values of Young's Modulus are similar for all the fibres tested regardless of their tensile strength.
2. The tensile strengths of crocidolite and chrysotile samples tested are on average similar.
3. The tensile strengths of the amosite fibres tested are lower than those found for the crocidolites and chrysotiles.
4. The tensile strength of the anthophyllite sample tested is very much higher than figures generally quoted

From Table II the following points emerge:-

1. The values of Young's Modulus do not appear to vary with the temperature to which the fibre has been heated.
2. Neither the amosite nor the crocidolite lose any strength up to about 200°C.
3. Both the amosite and the crocidolite have lost 50% of their strength at about 350°C.
4. At 600°C the amosite retains only about 5% of its strength but the crocidolite still retains about 12% of its strength at 800°C.

Work is at present in hand to produce similar tensile strength/temperature data for chrysotile. Preliminary tests indicate that chrysotile retains all its tensile strength up to at least 400°C, but the strength diminishing by about 80% at 600°C. It is hoped to complete this work in time for it to be presented at the conference.

REFERENCES.

1. Zukowski R, Gaze R., Nature, Lond., 1959, 183, 35.
2. Marsh D.M.J. Sci. Instrum. 1961, 38, 35.
3. Hodgson, A.A., Freeman, A.G., and Taylor, H.F.W., Mineral. Mag., 1965, 35, 5.
4. Cilliers, J.J., Freeman, A.G., Hodgson, A.A., and Taylor, H.F.W., Econ. Geol. 1961. 56, 1421.
5. Hodgson, A.A., Freeman A.G., and Taylor, H.F.W., Mineral. Mag. 1965, 35, 445.
6. Hodgson, A.A., 'Fibrous Silicates'. The Royal Institute of Chemistry, Lecture Series, 1965, No. 4., 14-17.
7. Hodgson, A.A., Mineral. Mag., 1965, 35, 291.
8. Ahlfeld, F., Notas. Mus. La. Plata., 1943, 8, 355.
9. Aurola, E., and Vesassalo A., 1954, Geologinen Tutkimsulaitoo Geotekmillisia Julkaisuja No. 54, Helsinki.

TABLE I.

Ore Samples	No of Tests	Youngs Modulus	Coefficient of Variation	Tensile Strength	Coefficient of Variation	Average Cross-Sectional Area of Fibres Tested.
		$x10^6$ lbs/in^2	%	$x10^3$ lbs/in^2	%	x 10^{-6} cm^2
idolite, Koegas, Cape Province (3) (4)	20	21.2	8.7	411	13.9	1.65
idolite, Koegas, Cape Province (3) (4)	20	21.8	9.3	448	11.5	1.33
ite, Penge, Transvaal (5)	20	20.6	3.0	372	9.1	2.71
ite, Penge, Transvaal (5)	20	20.6	5.6	286	15.4	1.83
sotile, Arizona, U.S.A.	20	20.8	4.3	547	11.7	2.07
sotile, Thetford, Canada (6)	20	21.0	8.2	527	12.4	2.13
idolite, Pomfret, Cape Province (7)	10	24.4	5.2	674	9.8	1.64
idolite, Pomfret, Cape Province (7)	10	25.2	8.3	511	14.1	1.34
idolite, Cochabambo, Bolivia (8)	4	24.5	-	208	-	2.43
ophyllite, Paakilla, Finland (9)	10	22.5	8.3	353	28.0	0.95
ed Asbestos Fibres.						
ite, Malips, Transvaal(6)	10	22.4	9.1	210	10.4	2.64
ite, Penge, Transvaal	8	23.0	7.3	407	21.6	1.13

Descriptions of above materials are given in the referenced papers.

2-8 (4) TABLE II.

Ore Samples	Temp °C	No. of Tests	Youngs Modulus	Coefficient of Variation	Tensile Strength	Coefficient of Variation	Average Cross-Sectional Area of Fibres Tested
			$x10^6$/lbs/in^2	%	x10^{3}lbs/in^2	%	x 10^{-6} cm^2.
e, Penge (2)	20	10	20.6	3.0	372	9.1	2.71
"	210	10	21.9	7.0	377	11.5	1.59
"	250	10	22.4	4.3	313	9.6	2.04
"	310	10	21.3	6.4	226	15.6	1.13
"	390	10	22.1	5.8	154	15.3	3.00
"	495	10	21.6	5.4	73	13.6	5.30
"	600	10	17.6	18.3	19	20.1	30.81
olite Pomfret(7)	20	10	24.4	5.2	674	9.8	1.64
"	150	10	25.8	3.1	689	9.2	1.37
"	210	10	25.5	9.7	669	13.9	1.06
"	250	10	25.1	2.9	653	10.0	1.67
"	310	10	25.0	6.9	547	15.9	1.74
"	390	10	24.2	10.4	279	15.3	2.35
"	495	10	26.1	5.3	151	10.7	3.26
"	600	10	25.7	3.4	126	20.9	2.60
"	800	10	23.9	14.5	81	57.8	2.50

The samples were maintained at the stated temperatures (in a stream of oxygen) for a period of 4 hours.

2-9: Fundamental Investigations of Asbestos Reinforced Cement

by

L. de Mahieu
S.A. Eternit, Kapelle-op-den Bos (Malines), Belgium.

Experimental work has proved that, contrary to present ideas, the strength σ of asbestos-cement equals the product $c.\Omega$ of (c) the tensile strength of cement by (Ω) the actual fracture area, taking into consideration the fact that the rupture path goes around the fibres.

If the asbestos fibres in the material are all parallel to a direction φ,θ, which is the same as the breaking force, then Ω can be deducted from the Poisson formula. This formula determines :

- the number $n\, e^{-klz_{\varphi,\theta}}$ of cells not crossed by fibres in the unit area of the fracture section perpendicular to the φ,θ direction and
- the number $n\, klz_{\varphi,\theta}\, e^{-klz_{\varphi,\theta}}$ of cells crossed by one fibre.

It is understood that $K_{\varphi,\theta}$ is the number of fibres per unit of weight of asbestos, $l_{\varphi,\theta}$ the average length of these fibres, and the number of cells per unit of breaking section, $z_{\varphi,\theta}$ the weight of fibres in one cm3 of asbestos-cement, and $klz_{\varphi,\theta} = \frac{K_{\varphi,\theta}}{n}\, l_{\varphi,\theta}\, z_{\varphi,\theta}$.

The remaining cells crossed by several fibres have a negligible strength.

Knowing that the cells of cement have a tensile strength $\frac{c}{n}$ and that the cells crossed by one fibre have a strength $2\pi\rho r\frac{1}{2}c$ it comes :

$$\sigma = c\,(e^{-klz_{\varphi,\theta}} + \pi\rho r \ln klz_{\varphi,\theta}\; e^{-klz_{\varphi,\theta}})$$

When the fibres are at an angle ψ with the direction of the stressing force α, the number of fibres crossing the fracture area is lower and the modified formula becomes :

$$\sigma' = c\left[1-(1-e^{-klz_{\varphi,\theta}} - \pi\rho r \ln klz_{\varphi,\theta}\; e^{-klz_{\varphi,\theta}})\cos\psi\right]$$

from which we derive, after integrating for all the fibres, the general equation :

$$\sigma_t = \int_{\theta=-\frac{\pi}{2}}^{\theta=+\frac{\pi}{2}} \int_{\varphi=\alpha-\frac{\pi}{2}}^{\varphi=\alpha+\frac{\pi}{2}} \frac{c}{2\pi} \left[1-\cos\theta\cos(\varphi-\theta)\left(1-e^{-klz_{\varphi,\theta}}-\chi\rho r\ln klz_{\varphi,\theta}e^{-klz_{\varphi,\theta}}\right)\right] \cos\theta \, d\varphi \, d\theta$$

This equation shows characteristic curves already experimentally established.

The value of parametres in equation σ_t , must be determined. It should be noted that the blaine $B = \frac{2\omega}{\rho' r \delta}$ permits to find the radius $\rho' r$ of the "bundles", if density δ of asbestos is known and if $\omega = \frac{\rho' r}{\rho' a r}$ is the ratio of the bundles radii respectively in the air and in the asbestos-cement.

On the other hand the distribution of the number of fibres according to their length is log-normal, sothat the distribution function of the reduced normal law reads :

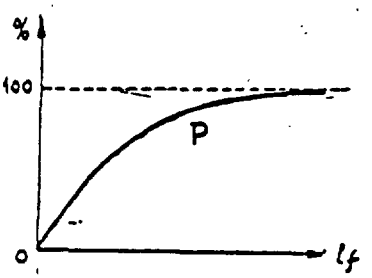

$$P = \int_0^{\infty} N l_f \, dl_f = \Phi\left(\frac{\log l_f - \mu - \nu^2}{\nu}\right)$$

Then the average length of the fibres can be computed :

$$l_m = \frac{\int_0^{+\infty} N \, l_f \, dl_f}{\int_0^{+\infty} N \, dl_f} = e^{\mu + \frac{\nu^2}{2}}$$

Fibres which are too short, and dusts are unsuitable for making asbestos-cement. However there is a certain amount of these in every asbestos. On the other hand, some fibres are too long and this excess of length does not increase the strength of the product. Therefore

the length l should be expressed :

$$l = \frac{\int_{l_{ac}}^{l_{AC}} N l_f \, dl_f}{\int_{l_{ac}}^{l_{AC}} N \, dl_f}$$

where l_{ac} is the length below which a fibre should be regarded as dust and l_{AC} the length above the useful length.

To summarize, calculation shows that, for a given number of fibres the strength of a fibres reinforced cement product will be proportional to the length of the fibres and inversely proportional to their radius. The strength of the material can be increased if a thicker matrix of cement adhering to the fibres can be obtained.

It is also possible to compute the length of the fibres to be used in manufacturing fibre-cement product. This length must remain between the limits l_{ac} and l_{AC} . With the cumulative curve P obtained from the Mac Nett test, the Henry straight lines can be established, giving for a shipment of asbestos the proportion of fibr s having a suitable length

These lines show furthermore the amount of length reduction of the fibres bundles resulting from the different processes of milling.

The Blaine measurement gives the radius of the bundles. It also permits to determine the action of the milling operation on the radius.

The two tests normally performed by asbestos-cement manufacturers give the characteristics of asbestos. By working these characteristics into the general equation of asbestos-cement, it is possible to predetermine, by calculation, the strength σ of the product.

2-10: Measurement of the Surface Area of Asbestos Fibres.

by

A.A. Hodgson[1] and A. White[2],
1. Cape Asbestos Fibres Limited,
Harts Lane, Barking, Essex.

2. Department of Chemistry,
The University of Nottingham,
University Park, Nottingham.

The surface areas of 21 selected samples of asbestos fibre, as used in practice, have been compared by means of Rigden air permeability measurements and BET (Nitrogen absorption) measurements. For amosite and crocidolite there is a reasonably constant ratio between the BET surface areas and the air permeability surface areas, measured at room temperatures, these being:-

$$\frac{\text{BET S.A.}}{\text{Air Perm. S.A.}} \quad \text{(Crocidolite)} = 2.6 \text{ mean}$$

$$\frac{\text{BET S.A.}}{\text{Air perm S.A.}} \quad \text{(Amosite)} = 2.1 \text{ mean.}$$

Such a relationship does not exist for the chrysotile samples. Seven samples showing sucessively higher surface areas by air permeability show little variation in surface area as measured by BET. This suggests that nitrogen penetrates fibre bundles to such an extent as to indicate an ultimate surface area regardless of the degree of fiberisation of the bundles. It is therefore not possible to find any satisfactory relationship between 'true' and 'apparent' surface areas for chrysotiles.

Sample	Series	SURFACE AREAS m^2/gm				S.A. RATIOS		
		Air Perm room temp (1)	BET outgas room temp (2)	BET outgas 100°C (3)	BET outgas 200°C (4)	Col 2 Col 1 (5)	Col 3 Col 1 (6)	Col 4 Col 1 (7)
Chrysotiles								
No. 1	B	0.63	16.83	17.91	18.40	26.7	28.4	29.2
2	A	0.96	9.03	13.65	14.21	9.4	14.2	14.8
3	B	1.16	15.77	16.07	16.39	13.6	13.9	14.1
4	B	1.40	13.75	14.52	14.06	9.8	10.4	10.0
5	B	1.64	14.22	15.27	16.42	8.7	9.3	10.0
6	A	1.86	8.53	12.90	12.90	4.6	7.0	7.0
7	B	2.02	14.92	15.20	16.17	7.4	7.5	8.0
Crocidolites								
No. 8	B	0.64	1.90	2.33	2.55	3.0	3.6	4.0
9	B	0.78	1.70	1.79	1.79	2.2	2.3	2.3
10	B	1.04	3.15	3.28	3.50	3.0	3.2	3.4
11	A	1.13	3.61	3.91	4.00	3.2	3.5	3.5
12	B	1.40	3.21	-	3.47	2.3	-	2.5
13	A	1.70	4.17	4.78	5.08	2.5	2.8	3.0
14	B	3.49	7.61	8.46	9.34	2.2	2.4	2.7
Mean Ratios		-	-	-	-	2.6±0.4	3.0±0.5	3.1±0.5
Amosites								
No. 15	B	0.57	1.14	1.08	1.32	2.0	1.9	2.3
16	B	0.81	1.39	1.56	1.67	1.7	1.9	2.1
17	A	0.92	2.95	2.89	3.30	3.2	3.1	3.6
18	B	1.22	2.59	2.54	3.06	2.1	2.1	2.5
19	B	1.35	2.14	2.43	3.07	1.6	1.8	2.3
20	A	1.54	3.32	3.83	4.08	2.2	2.5	2.7
21	B	2.50	4.42	4.91	5.44	1.8	2.0	2.2
Mean Ratios		-	-	-	-	2.1±0.4	2.2±0.4	2.5±0.3

3-1: The Origin of Chrysotile Asbestos in Southern Africa.

by

D.H. Laubscher
New Amianthus Mines (Pty) Limited,
209, New Commercial Exchange Buildings
7, Harrison Street,
Johannesburg, South Africa.

Chrysotile asbestos deposits are found in the majority of the Archean ultramafic bodies in Rhodesia and South Africa, as well as in the Proterozoic dolomites in South Africa and Botswana.

Whilst chrysotile asbestos is a very common, widespread mineral, economic deposits are confined to certain ultramafic bodies and to specific areas within those bodies. Six geologically different asbestos deposits will be discussed in terms of the mechanism for fibre growth and the major controlling factos in fibre formation.

A. Fibre Growth Mechanism.

Three distinct growth mechanisms are apparent and the chrysotile fibre formed can be placed in the following categories:-

1. Stress Controlled Dilation Seams. The fibres in this category have formed in existing fractures in which the seam walls can be matched and inclusions in the fibre seam can be fitted to the seam wall. Fibre growth was only possible if the stress conditions at the time of formation were such that the load on the seam wall had been reduced so that the growing force of the fibres was sufficient to push the walls apart. The fibres are orientated at a large angle to the seam wall regardless of the attitude of the seam; this indicates that the walls did not move apart under tension. The material for fibre growth was either derived from the fracture wall during serpentinization e.g. Shabanie Mine; or from the host serpentinite going into solution e.g. King and Amianthus Mines.

2. Recrystallisation of Serpentine to Fibre. Slip fibre and certain cross fibre seams fall into this category. The longer slip fibres are localised in planes along which mild shearing has taken place and the stress across the plane was of the required magnitude. The serpentine has recrystallised to chrysotile fibre, with the fibre orientated in the direction of movement.

The cross fibre seams are characterised by

(1) fibres grading into the host rock,
(2) the colour of the fibre similar to the host serpentine,
(3) incipient lenticular fibre seams,
(4) a parallel orientation of the fibres regardless of the altitude of the seam wall and
(5) fibre development related to minor structures in the seam or it's immediate vicinity.

areas subjected to a steadily maintained stress. Examples of cross fibre deposits of this type are: Sheffield claims, Amianthus Mine and the dolomite deposits.

3. Replacement Fibre. This form of fibre growth is extremely common as a result of serpentinisation of olivine. The fibre replaces the olivine by outward growth from crystal boundaries and fractures. The fibres rarely exceed 2m.m. in length, with the direction of growth and length bearing a relationship to the spacing and arrangement of the initiating surfaces. This mechanism does not give rise to the economic fibre seams

B. CONTROLLING FACTORS.

The main controlling factors in the formation of economic deposits of chrysotile asbestos are:-

1. Host Rock Control. In general fibre seams are confined to those rocks that (a) have the same composition as the chrysotile fibres, viz. the green serpentinites and serpentine bands in the dolomites, (b) are composed predominantly of olivine i.e. dunites and peridotites. These are rocks which will readily provide magnesium and silica as material for fibre growth or will recrystallise to fibre in situ.

2. Serpentinous Solutions. The term serpentinous solution is used to denote a solution containing magnesium and silica from which serpentine minerals can form. The serpentinisation of olivine by hydrothermal solutions results in excess magnesium and silica going into solution to form the serpentinous solution.

$$5Mg_2SiO_4 + 4H_2O - 2H_4Mg_3Si_2O_9 + (4MgO + SiO_2)$$

Olivine	Introduced Water	Serpentine	Removed in Solution	
(700gm:219c.c)	(72gm)	(552gm:220 c.c.)	(160gm)	(60gm)

Therefore in the partially serpentinised dunite, as at Shabani, the presence of hydrothermal solutions was essential. In the serpentinite, e.g. 'King and Amianthus Mines, the serpentine appears to have gone into solution in areas of pressure, with hydrothermal solutions assisting with the process.

3. Structural Control. The main features in structural control are:-

(a) The formation of fractures in which stress controlled dilation seams can form and from which serpentinisation can take place. The fractures might predate the major structures in the area e.g. Shabani, or be contemporaneous e.g. King and Amianthus.

(b) The development of thrust faults, wrench faults and shear zones. These would act as channelways for hydrothermal solutions or have areas of pressure where serpentine could go into solution. Associated with the faulting would be areas with a suitably-orientated minor principal stress direction for the formation of stress controlled dilation seams. It is significant that fibre is best developed in those areas that have the simplest structural pattern.

(c) In areas where wrench faulting was dominant slip fibre is localised in the fault zone or sypathetic structures.

(d) The presence of certain structures which create the correct stress environment, allowing serpentine minerals to recrystallise to form fibre seams.

Cilliers J.J. le R. and Genis, J.H. (1964).Crocidolite Asbestos in the Cape Province. The Geology of Some Ore Deposits in Southern Africa, geol. Soc. S. Afr.

by

A.A. Hodgson
Cape Asbestos Fibres Ltd.,
Harts Lane, Barking, Essex.

The South African amphibole asbestos minerals, crocidolite, $Na_2Fe_2^{+++}Fe_3^{++}Si_8O_{22}(OH)_2$, and amosite, $Fe_{5.5}^{++}Mg_{1.5}Si_8O_{22}(OH)_2$, occur in metamorphosed sedimentary rocks containing up to 40% iron oxides by analysis. These ferruginous rocks known as Banded Ironstones form part of the Transvaal system, an extensive outcrop of strata, which stretches in a broad arc of some 800 miles from Northern Cape Province through the south eastern corner of Bechuanaland and as far as Eastern Transvaal.

The only known occurrences of amosite asbestos lie in a 40 mile arc spanning the Olifants River in E. Transvaal. The richest deposits occur on the farms at Penge, Weltevreden, Kromellenborg, at the Southern end of this arc; and at its westerly end at Malipsdrift there is a remarkable development of doublet veins of amosite and crocidolite.

In the Transvaal the immense Bushveld Igneous complex has intruded the rocks of the Transvaal System. It is thought that this intrusion may have promoted the formation of amosite, but there is no evidence that igneous activity has been essential for the formation of fibrous amphiboles in general throughout these sedimentary rocks.

With regard to the origin of the amphibole asbestos of South Africa, du Toit[1] considers that amosite and crocidolite were developed from original ferruginous clays which absorbed soda where necessary from their marine environment. These clays compacted during the deposition of overlying sediments of later systems, and a random orientation of fine fibres developed in much of the rock (mass fibre). Subsequent folding of all these strata controlled the development of cross fibre asbestos seams, the fibre growth being orientated at right angles to the direction of pressures which caused the folding.

More recently Cilliers and Genis[2,3] have considered the events leading up to sedimentation of materials in the Transvaal sea, with particular respect to crocidolite. The solution, transport and precipitation of iron and silica from the surrounding land into the sea was controlled by both chemical and biochemical means. Biochemical action coupled with a primitive algal life preserved a ferrous/ferric iron balance through the maintenance of the correct oxidation-reduction potentials. Iron compounds and colloidal silica transported to marine basins were then precipated under more alkaline conditions generated by the underlying dolomite. Layered precipation was further governed by changes in composition and temperature. Among the primary minerals crystallising out of these sediments, magnetite is considered to be of great importance; randomly distributed magnetite crystals seeded mass-fibre while cross fibre seams were seeded from layers of magnetite.

The generation of amosite presents further problems. The Banded Ironstone sediments of the Transvaal system must have contained copious amounts of organic muds. Evidence of primitive forms of life has been found in the Dolomite underlying the Banded Ironstones, in the form of massive concretions associated with algae. Du Toit reported similar structures of the Collenia type and traces of other fossils in the Banded Ironstone of the Kuruman area. (1). The bulk of their products of decay would have been dissipated in the earliest states of consolidation of the sediments leaving only a tiny residue of primitive oils in their trail. The present day yield of primitive oil from Cape Province crocidolite varies from trace amounts to 200 mgm/100gm. fibre, and that from the Transvaal amosite varies from trace amounts to 20 mgm/100gm fibre.(4) It is relevant that so much more oil has been found in crocidolite than in amosite. In the amosite fields of the Transvaal the process of decay appears to have been interrupted by a more violent form of decomposition. Unlike the asbestos horizons of Cape Province, the host rocks of amosite contain considerable amounts of carbon and sulphur. Typical analyses of rocks from Penge, Transvaal, give up to 6% carbon as graphite and up to 2.5% of combined sulphur. The graphite occurs both as thin layers in the banded strata and disseminated as a fine dust through selected bands which may be dominated by grunerite crystals, amosite fibre or iron magnesium carbonates.

It is supposed that the carbon and sulphur are the result of thermal degradation of organic matter due to heating up of the sedimentary strata by the Bushveld igneous intrusives. Under these conditions all the iron in the sediments was reduced to and held in the ferrous state. The process seems to have commenced prior to the stage of incipient crystallisation of the amosite, and there is evidence that fibre formation was complete before the termination of the igneous activity. In the final metasomatic stages associated with the intrusion hydrothermal solutions carrying up CO_2, presumably from decomposition within the underlying dolomite, have altered many patches of amosite fibre in their seams to an iron magnesium carbonate (ankerite).

Had the Bushveld intrusion never taken place amosite may not have been known, and crocidolite may have been found in its stead. The key to this suggestion lies in the Malips River area, some miles north of the amosite fields. In this area crocidolite is intimately associated with amosite both in that seams of amosite and crocidolite occur in the same reef, and in that crocidolite seams themselves often have a thin selvedge of amosite, usually at one edge of the seam only. Here the degree of thermal metamorphism imposed by the Bushveld intrusion may have been insufficient to bring about complete reduction of all the iron in the sediments to the ferrous state. This may have been assisted by the thin dissemination and layering of carbonaceous matter in this particular locality so that there was insufficient present for the reduction of all the ferric iron. Certainly graphite is absent from these rocks.

This paper will be illustrated by slides of typical thin sections of Amosite and associated rocks from Penge and Kromellenborg, and of amosite/crocidolite doublets from Malipsdrift.

REFERENCES.

1. DuToit, A., 1945. Trans Geol. Soc. S.A., 48, p.161.
2. Cilliers, J.J., Genis J.M., 1964, The Geology of some ore deposits of South Africa, Vol. II, Geol Soc. S.A.
3. Cilliers, J.J. 1961., D. Sc. Thesis, Pretoria University.
4. Harington, J.S., 1962, Nature, 193, p.43.

3-3: The Crocidolite Bearing Rock of Cape Province, South Africa.

by

N.W. Poulter
North Nottinghamshire College of Further Education,
Nottingham

Seams of Blue Asbestos (Crocidolite) occur interbedded in the Banded Ironstone zone of the Lower Griquatown stage of the Transvaal system. The outcrop of this system is virtually continuous along a 300 mile front extending in a N-S direction from the Orange River in Cape Province to the Bechuanaland border. The Transvaal rocks occur in a series of interconnected shallow basins. Crocidolite is sporadically developed throughout these horizons but the formations are believed to be discontinuous and payable deposits are comparatively sparse.

The crocidolite-bearing rock is described as the horizons are traced northwards. This trace is represented by three locations. Koegas-Westerberg (near Prieska) in the south, Warrendale in the Danielskuil - Postmasberg area some 50 miles south of Kuruman and Pomfret in the north near the Bechuanaland border.

Based on extensive petrological examination and thin section work the mineralogy and textures exhibited by these rocks are compared and contrasted. The diagnostic features of the South African crocidolites in thin sections are described emphasizing the criteria that distinguish them from crocidolites that have grown within different environments.

Attention is primarily focused on the crocidolite and its relation to associated riebeckite both in forms and structures. Cilliers and Genis tended to categorize the crocidolite and riebeckite into two genetic divisions (mass-fibre riebeckite and perfectly orientated cross-fibre crocidolite) but the evidence suggests that they are a genetic whole. Every gradation has been found between the randomly-orientated riebeckite fibrous needles to perfectly orientated cross-fibre crocidolite to confirm this supposition. The inter-relations of the crocidolite - riebeckite will be seen to vary as the locations are traced northwards due to the interesting factors of change of chemical environment and degree of metamorphism.

These two influences are also reflected in the associated mineral assemblages. The inter-relation of the magnetite-quartz-calcite-minnesotaite-stilpnomelane-chlorite complex found towards the south are described and are found to give way to a more distinctly arenaceous assemblage to the north with marked changes in structure and form. Most notable is the disapearance of minnesotaite and the predominance of silica. Further, primary hematite makes its appearance. The implications for environment of deposition are discussed notably that a predominently non-argillaceous localised environment has

not hindered the development of riebeckite and crocidolite. This does not support the view of Cilliers and Genis that riebeckite was formed in situ by simple dehydration and slight ionic reorganisation of clay minerals. Their optical work was based solely on the asbestos bearing rocks of the Abramsdam Syncline in the Westerberg-Koegas area where the present work has confirmed that the environment of the rock in immediate association with the riebeckite and crocidolite is predominantly argillaceous.

The evidence for the affects of regional metamorphism and its extent are discussed. In a general way it is possible to relate the direction of fibre growth with pressures at right angles to the growth, associated with folding. It is self evident that these pressures were not equally distributed and that a heterogenity of structures of riebeckite and crocidolite have resulted.

Other riebeckite and crocidolite structures which cannot be reconciled with the stresses due to folding of these rocks can be related to hydrostatic pressure and pressure due to the overburden.

These pressures can also be seen to have had their effect on the extra mineral assemblage (foliation structures) for example) and the effect is particularly pronounced in the recrystallised and frequently orientated quartz.

It is believed that the origin of crocidolite is fairly well understood although there exists some controversy on control of growth. There is not enough evidence to support or weaken the view that the crocidolite crystallised in situ from the lithification of material precipitated chemically and biochemically in large shallow basins.

However, it is suggested that, contrary to Cilliers and Genis, although the precipitated material provided the source for the genesis of crocidolite, there is evidence to indicate that crocidolite is a stress mineral and its fibrous nature is related to dynamic metamorphism. The effects of regional metamorphism as well as other pressures (Hydrostatic and that due to the overburden) can be seen in all the locations examined of the asbestos bearing rocks of the Lower Griquatown stage. It is further suggested from the evidence that low grade regional metamorphism has been an essential factor in the genesis of the crocidolite from riebeckite parentage. The evidence confirms that an initiating surface of magnetite (Cilliers and Genis) is not paramount to the growth of crocidolite but rather may be a secondary factor that facilitates growth of perfectly-orientated cross-fibre crocidolite.

It is accepted that riebecite and the associated mineral assemblage may be derived from chemical precipitates as primary minerals but their present form is 'secondary' due to recrystallisation due to the influences of various pressures, notably regional metamorphism.

To enable a complete picture of these rocks to be presented they will be briefly contrasted with the crocidolite of the E. Transvaal which occurs in very close association with the Amosite. It will be noticed how the effects of thermal metamorphism due to the intrusion of the Bushveld Igneous complex has accentuated certain forms and structures.

The text of the lecture will be based on a continuous series of coloured photo-micrographs of thin sections taken on microscopy equipment of the Cape Asbestos Co. Ltd., in their Laboratory at Barking, Essex.

Reference :-

Crocidolite Asbestos in Cape Province. Cilliers and Genis, (The Geology of some ore deposits of South Africa, Vol. II 1964. Published by Geol. Soc. S.A.)

3-4: Mineralogy of the Coalinga Asbestos Deposit

by

F.A. Mumpton and C.S. Thompson
Union Carbide Corporation, Mining and Metals Division,
P.O. Box 579, Niagara Falls, New York 14302, U.S.A.

Since 1960 the asbestos production of the United States has more than doubled, a phenomenon in large part due to the development of the Coalinga asbestos deposit in western California. Despite the fact that this deposit is of enormous size and contains over 50% recoverable fiber, it remained unrecognized for over 100 years, since its physical appearance is totally unlike that of almost every other asbestos deposit in the world. The Coalinga deposit occupies the southeastern third of the New Idria serpentinite, an elongated dome-shaped body about 4 miles wide and 12 miles long, which has been intruded into greywackes and shales of Jurassic and Cretaceous age. Whereas most asbestos ores consist of cross-fiber veinlets of chrysotile within massive serpentinite, no such veinlets have been found in the Coalinga deposit. This body has been extensively sheared and pulverized into a gigantic pile of powdery asbestos. The great bulk of the deposit consists of soft, powdery, pellet-like agglomerates of matter, friable chrysotile, surrounding blocks and fragments of hard, dense, competent serpentinite. The very nature of this ore has led directly to its exploitation, since mining can be accomplished with ease, by low-cost, open pit methods, and the fiber content can be easily separated from the coarse, hard rock. At the present time three companies are processing Coalinga ore with an annual production of about 50,000 tons.

Four main types of serpentine materials are distinguishable in the ore: (1) fragments and blocks of hard, dense serpentinite, ranging in size from fractions of an inch to boxcar dimensions; (2) large, tough, leathery sheets of matted chrysotile, up to several square feet in size; (3) brittle, bladed fragments of green serpentine, up to several square inches in size; and (4) soft, friable, greenish-white agglomerates of flaky asbestos, 1/4" to 1" in diameter, which also contain appreciable amounts of both the green, bladed material and the hard, gritty serpentinite. The bulk ore consists predominantly of members of the serpentine group, with chrysotile making up about 75% of the total. Chrysotile is almost the sole constituent of both the green bladed material and the leathery sheets. Serpentinite fragments consist primarily of lizardite and antigorite, with smaller amounts of short-fiber chrysotile, brucite, and magnetite. Minor quantities of calcite and traces of chromite and uvarovite are also present. Talc has not been observed.

Coalinga chrysotile has an unusually large surface area, about 70-80M^2/g, most likely due to the absence of inter-fiber material, compared with most other chrysotiles. Although long-fiber, per se, is not present, fiber lengths up to several microns have been noted in the leathery sheets. Most of the chrysotile in the ore, however, is much shorter and is arranged in a swirling mesh of disoriented, tangled fibers, much like cellulose in paper. Serpentinite gangue is scattered throughout the soft ore, and contains the bulk of the platy serpentines present. Petrographically it is not unlike most other serpentinites; however, brucite is a common constituent and is often found intimately intergrown with serpentine. The results of chemical, electron probe, and X-ray analyses confirm that the brucite of this ore is iron-rich, having an approximate formula of $(Mg_{10}Fe2)(OH)24$. The high iron content of the brucite is a critical factor in the susceptibility of the ore to weathering, and brucite-rich ore invariably discolours rapidly when exposed to surface oxidation conditions. Within the 20-30' thick surface weathering zone, blocks and fragments of brucite-rich serpentinite transform into dark brown, soft, crumbly masses. The weathered serpentinite 'boulders' are enriched in pyroaurite, the new mineral, coalingite, and amorphous iron oxides, while brucite is almost absent. Laboratory experiments have confirmed that in the surface weathering zone, iron-rich brucite either dissolves, leaving behind a residue of brown, amorphous iron oxides, or transforms in situ into pyroaurite or coalingite by oxidation and carbonation. The dissolved magnesium later precipitates as hydromagnesite which is abundant immediately above the water table throughout the deposit.

The presence of about 8% brucite in the New Idria serpentinite suggests that the parent igneous rock was a dunite, which was injected into the surrounding sediments during the serpentinization process. Its location, a few miles east of the famous San Andreas fault zone, probably accounts for its extremely sheared and fractured nature. The material present in the mass today may be the result of intensive crushing and pulverization during or after serpentinization, much as a thick paste is ground and smeared in a wet ball mill or mix-muller. The abundance of chrysotile, especially in the friable portions of the ore, may be the result of lizardite and antigorite of the original serpentinite transforming into the 'stable' phase, chrysotile, during this extensive reworking process.

by

J. Hruskovā[1] and J. Kourimskỳ[2]

1. Geological Survey, Hradebni 9, Prague.
2. National Museum, Prague.

It is the purpose of this paper to give a survey of the occurrences of the different types of serpentine asbestos in the territory of Czechoslovakia and of the present position regarding the investigation of these minerals. Special attention has been paid to our most important localities: Dobsinna (Slovakia), Kremze (S. Bohemia), Prisecnice (N. Bohemia), Marianske Laszne (W. Bohemia) and Letovice (Moravia).

First of all a mineralogical identification of the samples investigated was carried out. As the main method of identification X-ray diffraction was used. The chemical compositions were determined and a structural formulae calculated. There is a concise optical characteristic of the examined materials. The refractive indices of these samples were measured by means of the double variation method. The samples were also examined with the electron microscope. Special attention has been paid to the thermal study of serpentine asbestos. The specimens were subjected to differential thermal and thermogravimetric analysis, and their derivative thermogravimetric curves were obtained.

In the conclusion of the paper the data on the serpentine asbestos specimens, obtained by means of X-ray methods, thermal study, chemical analysis, and optical study, are summarized and mutually compared.

Synthetic fibrous fluoro-amphiboles and their properties.

by
R.F. Grigorjeva, O.G. Chigarjova, and A.D. Fedoseev.
Institute of Silicate Chemistry,
USSR Academy of Sciences, Leningrad.

The problem of production and practical use of inorganic polymers, to which synthetic fibrous silicates of an asbestos type can be assigned, deserves increasing attention from both scientists and engineers. Systematic investigations of the conditions of synthesis, mechanism and kinetics of formation of fibrous silicates, and also the investigation of isomorphism and interrelation between the composition, structure and properties of these artificial minerals have been recently carried out at the Institute of Silicate Chemistry of the USSR Academy of Sciences in Leningrad. One of the trends of the mentioned investigations is the pyrogenetic synthesis of fibrous fluoro-amphiboles and investigation of the products.

The synthesis has been carried out by heating the initial mixtures of chemically pure reagents at 900-1100°C in tightly closed platinum or ceramic vessels. The initial mixture consists of the oxides and fluorides, in proportions corresponding to the stoichiometric formula of the synthesized fluoro-amphibole but with some fluorine excess. In addition, fluxes in the form of alkali and alkali-earth metal carbonates and chlorides are introduced into the mixtures.

The phase compositions of the products and the morphological peculiarities of the amphibole crystals depend upon the chemical composition of the initial mixture, its fluorine content, and the temperature of synthesis. The product is an entangled-fibrous mass, containing up to 80 - 90% of fluoro-amphibole fibres (length 0.5-1.0 mm, diameter 0.1 - 2.0 μ.) A brush of crystals of the same fluoro-amphibole with lengths up to 15 - 20 mm and diameters of 1 - 20μ grows on the surface of this mass.

Extensive investigations of the isomorphous substitutions of the cations in the structures of the synthetic fluoro-amphiboles have been carried out. We have prepared and investigated various series of fibrous fluoro-amphiboles, in which the cation group 'x' is occupied by Li^+, Na^+, K^+, Mg^{2+}, Ca^{2+}, Sr^{2+}, or Ba^{2+} and the cation group 'y' contains Mg^{2+} along with Fe^{2+}, Fe^{3+}, Cr^{3+}, Cu^{2+}, Co^{2+}, Ni^{2+}, Mn^{2+} or Cd^{2+}

The characterisation of the synthetic fluoro-amphiboles has been performed on the basis of chemical analyses, thermal, optical petrographic, and x-ray investigations, together with electron microscopy and infra-red spectroscopy. We are investigating physicochemical and mechanical properties of the synthetic fibrous fluoro-amphiboles in comparison with some natural asbestos specimens. Table I gives main results of the investigations.

As can been seen from the presented data, the synthetic fibrous fluoro-amphiboles are superior in their main properties to the best varieties of natural asbestoses and in some respects (e.g., thermal resistance and mechanical strength) they are considerably superior. This fact favours future scientific and experimental progress in this field.

TABLE I. COMPOSITION AND PROPERTIES OF THE SYNTHETIC FIBROUS FLUORO-AMPHIBOLES

(i) Compositions and Names.

Ref.	Composition Chemical formula.	Name
A	$Na_3 Mg_4 Fe^{3+} (Si_4O_{11})_2 F_2$	Mg-fluorarfvedsonite
B	$Li Mg_{6.5} (Si_4O_{11})_2 F_2$	Ti-fluoramphibole
C	$Na_2 Mg_6 (Si_4O_{11})_2 F_2$	Mg-fluororichterite
D	$Na_2 Ni^{2+}Mg_5 (Si_4O_{11})_2 F_2$	Ni-fluororichterite
E	$Na_2 Co^{2+} Mg_5 (Si_4O_{11})_2 F_2$	Co-fluororichterite
F	$Na_2 Mn^{2+} Mg_5 (Si_4O_{11}) F_2$	Mn-fluororichterite
G	$Na_2 Cu^{2+}_{0.5} Mg_{5.5} (Si_4O_{11}2 F_2$	Cu-fluororichterite
H	$Na_2Cd^{2+}_{0.5} Mg_{5.5} (Si_4O_{11})_2 F_2$	Cd-fluororichterite
I	$Na_{2.5} Mg_5 Cr^{3+}_{0.5} (Si_4O_{11})_2 F_2$	Cz-fluoramphibole
J	$Ba Mg_6 (Si_4O_{11})_2 F_2$ *	Ba-fluoramphibole

* An approximate formula is given.

(ii) Cell Parameters and Optical Properties.

Ref	Cell Parameters Å *				Optical Properties			
	a	b	c	β	n_γ	n_β	n_α	cn_γ
A	9.82	17.89	5.33	105°25'	1.630	1.623	1.618	20°**
B	18.16	17.68	5.37	90°00'	1.598	1.589	1.578	0°
C	9.66	17.92	5.26	102°59'	1.596	1.589	1.577	12°
D	9.65	17.91	5.26	102°43'	1.618	1.605	1.597	16°
E	9.67	17.96	5.26	102°48'	1.616	1.607	1.598	17°
F	9.71	17.94	5.26	102°51'	1.610	1.603	1.589	16°
G	9.66	17.92	5.26	102°48'	1.608	1.596	1.590	25°
H	9.72	17.96	5.26	103°12'	1,612	1.606	1.593	20°
I	not ascertained				1,618	1.608	1.594	20°
J	not ascertained				1,657	1.651	1.643	4°

**Parameter determination errors a,b,c,± 0.01 Å, β ± 5'
***The value of Cn_γ is given

(iii) Chemical and Thermal Stabilities and Mechanical Properties

Ref	Chemical stability:		Thermal stability:		Mechanical Properties:	
	weight loss(%) after 4 hours of boiling in		temperature range of		highest tensile strength	diameter of fibre investigated microns
	HCl sp.gr.1.19	KOH 25%	decomposition °C	melting °C	kg/mm²	
A	8.4	1.5	940-1000	1000-1060	366	0.8
B	33.5	3.5	860- 900	1090-1100	220	1.9
C	3.0	0.8	950-1000	1170-1190	210	3.4
D	9.1	0.7	960-1000	1070-1110	250	1.0
E	8.8	1.1	940-1000	1050-1100	364	1.6
F	15.5	1.9	990-1050	1140-1160	not ascertained	
G	not ascert		910- 970	1090-1125	"	
H	not ascert		920-1030	1070-1210	"	
I	11.3	4.0	1010-1070	1160-1190	400	" 1.6
J	not ascertained					

The Synthesis of Fibrous Amphiboles under Hydrothermal Conditions.

by

T.A. Makarova, L.N. Korytkova, and A.D. Fedoseev.
Institute of Silicate Chemistry,
USSR Academy of Sciences, Leningrad.

The hydrothermal synthesis of fibrous amphiboles, the investigation of their structure, composition and properties is one of the trends of the investigations carried out at the Institute of Silicate Chemistry of the USSR Academy of Sciences. The work is not only of purely scientific importance. The production of varying types of artificial asbestos of constant compositions and properties is of great practical interest because of their use as active sorbents and fillers.

Synthesis of fibrous amphiboles is carried out in autoclaves, using platinum and silver vessels, at 350° - 600°C and pressures of 300 - 2000 atmospheres. The initial components are mixtures of chemically pure reagents in the form of appropriate oxides, hydroxides, soluble salts, quartz, silica gel and also some natural magnesian silicates. The ratios of the initial components correspond to the stoichiometry of the synthetized amphiboles with a small alkali excess.

The formation of the fibrous amphiboles is greatly affected by the temperature, pressure, degree of dispersion of the initial components, the L:S ratio, the duration of the synthesis, and the pH of the medium. The duration of the synthesis can last from 6 hours to 3 days. As a rule, shorter times are used if the temperature is raised but in this case the thickness of the amphibole fibres increases.

The result of the synthesis is a adding-like elastic entangled-fibrous mass containing up to 95-98% of the thinnest amphibole fibres. The maximum length of the fibres is 3 - 4 mm, and their diameters are 10^{-4} - 10^{-5} mm.

Taking into account the peculiarities of the crystal structures of the amphiboles and their capacity for wide isomorphous substitution, we have synthesized several forms of fibrous amphiboles in which the 'X' sites are occupied by Na^{+} or Ca^{+}, and the 'Y' sites by Mg^{2+}, Fe^{2+}, Co^{2+}, or Ni^{2+}.

The characteristics of some synthetic fibrous amphiboles formed under hydrothermal conditions are shown in Table I. The results of the investigation thus show that under hydrothermal conditions it is possible to prepare fibrous amphiboles of various compositions and properties, and to a certain degree to model the processes which take place in the formation of asbestos minerals in nature.

3-7: (2) The Compositions and some Properties of the Synthetic Fibrous Amphiboles.

No.	COMPOSITIONS Chemical formula	PROPERTIES. Ng	Np	Ng-Np	Weight loss (%) after 4 hours of boiling in HCl, sp.1.19	Weight loss (%) after 4 hours of boiling in 25% KOH	Temperature of decomposition °C	Tempe of m °C
1.	$Na_{2.12}Mg_{5.45}(Si_4O_{11})_2(OH)_2$	1.591	1.573	0.018	16.20	5.00	770-780°	118
2.	$Na_2(Mg,Fe^2)_6(Si_4O_{11})_2(OH)_2$	1.636	..624	0.012	4.06	2.80	780-800°	115
3	$Na_{2.65}H_{0.23}Co_{5.52}(Si_4O_{11})_2(OH)_2$	1.660-1.682	..649-..666	0.011-0.012	16.99	5.10	750°	107
4.	$Na_{2.5}Ni_{5.65}(Si_4O_{11})_2(OH)_2$	1.672	..656	0.016	9.00	2.23	820°	120
5.	$Na_{1.8}H_{0.14}Ca_{1.05}Mg_{4.90}(Si_4O_{11})_2(OH)_2$	1.615	..600	0.015	10.25	1.76	840°	120

3-8: Investigation of the Quantitative Determination of Minerals in Serpentine Asbestos Samples by Infrared Spectroscopy and Thermoanalysis.

by
Edward Martinez, Robert B. Haagensen[1], and Harold L. Lovell[2].

1. Central Research Laboratories, American Smelting & Refining Co., South Plainfield, N.J.
2. College of Mineral Industries, The Pennsylvania, State University, University Park, Pa.

Although the minerals present in serpentine asbestos ore bodies may vary somewhat from deposit to deposit, the following are generally found in most:

Chrysotile	$3MgO.2SiO_2.2H_2O$	Brucite	$Mg(OH)_2$
Lizardite	$3MgO.2SiO_2.2H_2O$	Magnetite	$FeO.Fe_2O_3$
Olivine	$2(Mg,Fe)O.SiO_2$	Talc	$3MgO.4SiO_2.H_2O$

Since many of these minerals contain magnesium, iron and silica, a chemical analysis of an ore or fiber sample has only limited value in indicating the constituents present. The subject of this paper is the investigation into the use of infrared spectrophotometry (IR) and thermoanalysis for the quantitative determination of some of the minerals in chrysotile asbestos samples.

The sample preparation techniques for IR spectroscopy are discussed. Infrared spectra of chrysotile, lizardite, talc, olivine, brucite, and magnetite in the 2 to 15 micron and 11 to 25 micron ranges are presented. These spectra indicate that the most promising absorption bands for the various minerals that can be used for mineralogical determinations.

The use of an IR differential technique with pure chrysotile in the reference beam is shown to increase the sensitivity of the method. Examples with synthetic mixtures of chrysotile and talc are given.

It was found that the IR spectra of many of the minerals are much less complex after heating to certain temperatures. The possible application of heating the samples and reference prior to using the differential IR approach for the detection and quantitative measurement of talc is discussed, as well as the difficulties encountered in applying this procedure to olivine.

The semi-quantitative estimation of brucite and total serpentine (chrysotile and lizardite) by thermal gravimetric and differential thermal analysis is discussed.

3-9 THERMOGRAVIMETRIC ANALYSES OF SERPENTINE ASBESTOS AND RELATED MINERALS.

by

L.J. Monkman
Turner & Newall Ltd. Asbestos Fibre Laboratory,
c/o Turners Asbestos Cement Co. Ltd.,
Ashburton Road, Trafford Park,
Manchester, 17.

The studies were undertaken using a Stanton TR-02 Thermobalance of one-fifth milligram sensitivity, with specimens weighing one gram. (This weight ensures that representative results are obtained). A very slow heating rate, about 0.7°C per minute, was adopted as being the optimum for pyrolysis studies on serpentine asbestos. Determinations were made both with the asbestos decomposing in air in an open platinum crucible, and in a 'closed-chamber' crucible (constructed from Inconel 600) in which decomposition occurs in an atmosphere consisting mainly of the gases evolved. Investigation of the effect of variations in heating rate, specific surface area of the sample, and crucible geometry showed that the combination of slow heating rate (which minimises temperature differences within the specimen) and a 'closed-chamber' crucible reduces the effect of particle size and standardises the effects of crucible geometry. The design of the 'closed-chamber' crucible is based on that of P. D. Garn (Analy. Chem. 32, (1960) p.1563).

In order to provide semi-quantitative data on the accessory mineral content of asbestos samples, thermograms were obtained on specimens of cleaned chrysotile fibre, serpentine rock dust, and accessory minerals from mines in Africa and North America. The temperature ranges of decomposition so determined are shown in the table which follows.

Mineral	Major Decomposition Range* (°C) Crucible A**	Crucible B***
Chrysotile	475-725	525-725
Brucite	325-425	350-450
Magnesite	400-600	475-625
Calcite	625-825	800-975
Talc	700-1000	775-950

* Decomposition Range = range in which rate of loss per 25°C exceeds 1% of the total loss for that peak.

** Crucible A = platinum crucible, Johnson-Matthey Type UA 10 ml capacity

*** Crucible B = Inconel 600 'closed-chamber' crucible

The pyrolysis curve of chrysotile using the 'closed-chamber' technique shows three regions of weight loss. The first occurs between 75°C and 325°C and consists of loss of loosely bound water; the second, between 525°C and 725°C, represents loss of hydroxyl water and coincides with major breakdown of the chrysotile lattice. The third, occurring between 775°C and 925°C, is not fully explained but is thought to represent loss of a residual proportion of hydroxyl water from the lattic during recrystallisation into forsterite, which from DTA data is known to occur at about 810°C. The weight losses of the second and third peaks amount to about 90-91% and 5.0% respectively of the total loss occurring above 325°C; this relationship holds constant irrespective of the absolute value of the ignition loss, which varies for asbestos from different mines, e.g. Thetford Mines 12.96%, Swaziland 12.65%.

The accessory mineral content of asbestos samples is estimated by measuring the ignition loss over the appropriate decomposition range for each mineral, with small corrections for the presence of the other minerals. When the 'closed-chamber' technique is used the decomposition ranges are narrowed, and peak temperatures delayed so that peaks which would otherwise overlap are resolved. Overlap is not completely eliminated but is only troublesome where samples contain moderate to large amounts of carbonate minerals, in which event the carbonate content is checked by means of the Knorr Alkalimeter.

If the amounts of the various accessory minerals (plus magnetite) are added together, the remaining weight percentage is usually too large to be accounted for by the residual weight loss if this is assigned to fully hydrated chrysotile. The procedure which has been adopted is therefore to assume that the deficiency is caused by the presence of 'talcose minerals' with a combined water content of 4.75 per cent, as against 13.00 per cent for chrysotile. The quantitative assignment of chrysotile and 'talc' content is achieved by using a family of curves relating the residual weight loss to 'talc' and chrysotile content. It is interesting to consider to what extent the 'talcose minerals' are associated with the material located in the central capillaries of fibrils and perhaps also in the interfibrillar spaces.

$x(0.13) + y(.0475) = 13.$

$x + y = 1$

$13(1-y) + 4.75y = 13$

$12.96 = \frac{13 - 12.96}{8.25}$

0.5% talc